Albumin and fibronectin adsorption on treated titanium surfaces for osseointegration: An advanced investigation

Applied Surface Science 599 (2022) 154023

Contents lists available at ScienceDirect

Applied Surface Science

journal homepage: www.elsevier.com/locate/apsusc

Full Length Article

Albumin and fibronectin adsorption on treated titanium surfaces for osseointegration: An advanced investigation

J. Barberi [a,*], L. Mandrile [b], L. Napione [a], A.M. Giovannozzi [b], A.M. Rossi [b], A. Vitale [a], S. Yamaguchi [c], S. Spriano [a]

[a] Department of Applied Science and Technology, Politecnico di Torino, Corso Duca degli Abruzzi 24, 10129 Torino, Italy
[b] Chemical Physics and Nanotechnology Department, National Institute of Metrological Research, Strada delle Cacce 91, 10137 Torino, Italy
[c] Department of Biomedical Sciences, College of Life and Health Sciences, Chubu University, 1200 Matsumoto, Kasugai, Aichi 487-8501, Japan

ARTICLE INFO

Keywords:
Protein adsorption
Titanium
Surface modification
Hydroxylation
Surface characterization
Biomaterials

ABSTRACT

Protein adsorption has a central role in the outcome of implants. However, there is no consensus about the impact of the different surface properties on the material-protein interactions. Here, the adsorption of albumin and fibronectin in near-physiological concentration is investigated on three differently treated titanium-based surfaces and compared after a thorough characterization. The different titanium surfaces have very different surface properties, in particular regarding roughness, oxide porosity, wettability, surface energy, and zeta potential, which are all known to deeply affect protein adsorption. By merging several characterization techniques, some conventional and some innovative, it was possible to discriminate the effect of surface properties on different aspects of protein adsorption. Despite forming a continuous layer on all samples, the amount of proteins bound to the surface is mainly due to surface roughness and topography, which can overcome the effect of wettability and surface energy. On the other hand, the secondary structure of albumin and fibronectin and their orientation are determined by the hydroxyl groups exposed on the surfaces, depending on their surface concentration and acidic reactivity in the former, and the surface zeta potential in the latter.

1. Introduction

The enormous success of titanium as implantable material since the 30s is due to the suitable combination of mechanical and chemical properties, such as appropriate Young's modulus and a corrosion resistance bioinert native oxide layer [1,2]. Over the years, the research pushed towards surface modifications for better osseointegration [3,4]. A complete understanding of the protein adsorption process is one of the missing links toward the control of implant-bone interaction and reduction of implant failure, which is a current costly clinical issue [5,6]. Every medical device in contact with the biological fluids is rapidly covered by a protein layer, which forms a transient matrix as an interface for material-cell interactions [7]. Protein adsorption is a "common but very complicated phenomenon", as defined by Nakanishi et al. [8], that is played by several actors and affected by many different factors. The protein characteristics, parameters of the protein solution (composition, ionic strength, pH, temperature, protein concentration), and biomaterial surface properties are all intimately interconnected and their role is difficult to interpret [9–12]. The surface roughness and morphology, charge, wettability, free energy (SFE), hydroxylation and exposed functional groups can all deeply affect the type, amount, and conformation of adsorbed proteins. Great efforts have been put into understanding how proteins behave in contact with titanium-based materials [6]. However, there are still many dark areas that need to be highlighted and some disagreements between studies that need to be clarified. Generally, an increase in roughness after surface treatments is related to an increment of protein adsorption, in particular at the microscale, but the specific effect of different topographies is unclear [13,14]. Surface OH groups have also been related to increased protein adsorption by increasing the possible protein binding sites [15], even though the mechanism is still under discussion [16,17] and it must be clarified if the amount of OH groups or their chemical acid-basic reactivity plays a major role. The SFE has a contribution to the affinity of titanium surfaces towards proteins, but the different effects of the polar and the dispersive components remain unclear [18–21]. The role of surface charge is also widely recognized. Since the overall charge of

* Corresponding author.
E-mail address: jacopo.barberi@polito.it (J. Barberi).

https://doi.org/10.1016/j.apsusc.2022.154023
Received 31 March 2022; Received in revised form 8 June 2022; Accepted 18 June 2022
Available online 21 June 2022

most proteins is negative at the plasma pH (≈7.4), an increment of positive charges on the surface may increase the electrostatic interaction [22], while an increase in negative groups usually hinders protein adsorption [23]. Anyway, also negatively charged surface groups can interact with the positive protein domains [24]. In the case of positively charged proteins, the contrary happens. Besides the intrinsic complexity of protein and biomaterial properties interplay, which needs further investigation to be totally understood, there are other aspects of adsorption on titanium materials that need to be taken into consideration. As already observed by the authors, the use of a low concentration of proteins, as usually made in the literature, does not mimic the physiological environment [6]. The use of low concentrated solutions may exalt the differences among surfaces that might result negligible when it comes to near-physiological conditions [25,26]. Furthermore, new characterization techniques are needed to allow a comprehensive study of protein adsorption on surfaces of real clinical interest, not only on models or specifically prepared biomaterials [27,28].

The scope of the present work is to investigate and compare the adsorption of albumin (BSA) and fibronectin (FN) on titanium and Ti6Al4V alloy surfaces after different chemical treatments for increasing the bioactivity and osseointegration. Highly concentrated protein solutions, such as biological fluids, are used to evaluate if the effect of the surface properties can be significant in a physiological environment. The combination of several techniques, both conventional and innovative, here proposed by the authors, allows for obtaining significant information about how much proteins are adsorbed on the different samples or how they orient and change their 3D structure. By coupling these results with a thorough surface characterization of the materials, it was possible to correlate the effect of different surface properties on the adsorption mechanisms.

2. Experimental section/methods

2.1. Sample preparation

Titanium grade 2 (ISO5832-2, Nilaco Co., Tokyo, Japan) and Ti-6Al-4V grade 5 alloy (ASTM B348, Titanium Consulting and Trading, Buccinasco, Italy) were obtained as plate or bar (1 cm of diameter), cut into 10 × 10 × 1 mm square samples or 2 mm thick disks and polished using #400 SiC paper, washed with acetone and ultrapure water in an ultrasonic bath, respectively once for 5 min and twice for 10 min, and dried. Those substrates were subsequently subjected to three different chemical treatments in order to obtain bioactive metallic surfaces, as deeply described elsewhere [29–31]. Briefly, pure Ti plates were subjected to a mixed alkali-acid-heat treatment through a first soaking in 5 M NaOH solution at 60 °C for 24 h, then the second one in a 50 mM HCl solution at 40 °C for 24 h and to a final heat treatment at 600 °C for 1 h (reagents from Kanto Chemical Co., Inc, Tokyo Japan) [29]. In this work, these samples are labeled as Ti(A-HC-H). Ti alloy samples were subjected to two different treatments. The first one consists in soaking Ti64 plates in a 5 M NaOH solution and in a mixed solution with 50 mM $CaCl_2$ and 50 mM $SrCl_2$, at 60 and 40 °C respectively both for 24 h. Then the samples were heated at 600 °C and finally immersed in a solution containing 1 M $Sr(NO_3)_2$ and 1 M $AgNO_3$ (reagents from Kanto Chemical Co., Inc, Tokyo Japan) [30]. These samples are referred to as Ti64(SrAg). At last, Ti64 disks were treated by etching in HF- (Sigma Aldrich, St. Louis, USA) and subsequent controlled oxidation in H_2O_2 (PanReac AppliChem, Darmstadt, GE), according to a patented process [31]. Such specimens are named Ti64(HF- H_2O_2). As a control, polished up to #4000 grit Ti and Ti64 samples were used.

2.2. Biological reagents

Pure bovine serum albumin (powder) and fibronectin (lyophilized) (Sigma Aldrich, St. Louis, USA) were used as label-free proteins. Fluorescent-labeled proteins were also employed: tetramethylrhodamine (TMR)-conjugated BSA (Invitrogen, Waltham, USA) and rhodamine-conjugated FN (Cytoskeleton, Inc., Denver, USA).

2.3. Protein adsorption

Bovine serum albumin and fibronectin were solubilized in phosphate buffered saline solution (PBS; Sigma Aldrich, St. Louis, USA) in near physiological concentrations, 20 mg/ml and 0.2 mg/ml, close to blood plasma [32,33]. Protein adsorption was obtained by covering the sample surface with protein solution for 2 h at 37 °C, avoiding the evaporation of the solution. Then, they were rinsed with ultrapure water, dried under a laminar flow hood and stored in a fridge. Samples adsorbed with albumin have the suffix _BSA and samples with fibronectin, the suffix _FN.

For the KPFM and fluorescent measurement, specific adsorption protocols were developed. The surface shall be only partially covered by the proteins, to have an internal control in the potential image: a contrast is detected between the areas covered and uncovered by the proteins on the same specimen. Thus, just a small drop of protein solution was placed on the sample surfaces, and then they were incubated and washed as before. Fluorescent proteins came in a very limited amount, so the protein solution volumes were reduced. 10 μl of solution were placed on the sample and covered with a microscope coverglass and incubated in a humid chamber, to avoid evaporation, for 2 h at 37 °C. In order to avoid interferences in the fluorescent measurements, samples were thoroughly washed thrice in PBS and thrice in ultrapure water. Prior to observation and quantification, the samples were mounted with a mounting medium (Fluoroshield; Sigma-Aldrich) and another microscope coverglass.

2.4. Substrate characterization

Morphological characterization of the samples was performed by an optical profilometer (LSM900, ZEISS, Oberkochen, Germany) and topographical parameters were evaluated according to ISO 25178. The height maps obtained with the confocal microscope were analyzed by the software Confomap. The measurements were performed onto three different samples for each substrate.

Wettability and surface energy were also investigated. Static contact angle measurements were performed by the sessile drop technique at room temperature by means of an FTA 1000C instrument using water and hexadecane (Sigma Aldrich, St. Louis, USA) as probe liquids, whose surface tension is 72.1 mN m^{-1} and 28.1 mN m^{-1}, respectively. Three specimens for each surface were tested. The Owens-Wendt geometric mean method was employed to evaluate the surface energy and its polar and dispersive component [34].

Each of these values is reported as average ± standard deviation (SD).

2.5. X-ray photoelectron spectroscopy (XPS)

The different surfaces were investigated by XPS in order to obtain information on their chemical composition. Measurements were performed on samples prior to and after protein adsorption and also after the acid range of the zeta potential titration curves;

The chemical composition of the surfaces, before and after protein adsorption, was obtained by XPS measurements (XPS, PHI 5000 Versaprobe II, ULVAC-PHI, Inc., Kanagawa, Japan). A reference of BSA powder was analyzed as well. An Al-K source was employed and the take of angle was set at 45°. Survey spectra of the samples were collected to analyze the surface composition, while high resolution spectra were performed for the C1s and N1s region. The C1s peak was set as 284.8 ± 0.1 eV [35]. Peaks were deconvoluted by CasaXPS software. Peak fitting was performed using a Gaussian-Lorentzian (70–30%) curves and applying a Shirley and a linear background for the C1s and N1s peak respectively [36–38]. The full width at half maximum (FWHM) was restrained below 1.7 eV [39] and the peak positions were constrained in

a ± 0.2 eV range from BSA or literature references.

2.6. Protein quantification by chemical assay and fluorescent labeling

The bicinchoninic acid (BCA) protein assay (Thermofisher, Waltham, USA) was used to quantify BSA adsorbed on the various surfaces. BSA was detached by soaking in 300 µl of 2% SDS (Bioreagent Thermofisher, Waltham, USA) for 2 h and the producer protocol was followed to run the BCA protein assay. In order to obtain a reliable quantification of a very small amount of proteins, the range of the calibration curve was extended with respect to the one of the BCA kit: in particular, a linear correlation between albumin concentration and solution optical density was observed also in the range 0–10 µg. The standard calibration curve is reported in **Figure S3** (see Supporting information) The measurement was performed in triplicate with a blank control for each specimen and the number of proteins adsorbed was calculated with respect to the specimen surface area. The assay is based on the reducing capability of proteins towards Cu^{2+}, and the subsequent chelation of two molecules of BCA by Cu^{1+}, forming purple complexes. Since different proteins can reduce a different amount of copper ions, precise quantification of a certain protein is possible only if the calibration curve is obtained by using the same protein. Due to the availability limitation of fibronectin, only albumin was quantified with a BCA assay.

The number of proteins adsorbed onto the surfaces was also evaluated thanks to fluorescence intensity measurements. The fluorescent signal of conjugated proteins was acquired by ChemiDoc MP system (Bio-Rad), using the Rhodamine application (excitation source: green epi illumination; emission filter: 602/50 nm). The signal intensity was collected in the same area in each sample. Due to technical limitations, BSA and FN adsorbed samples were imaged separately.

2.7. Characterization of the protein distribution on the surface

The distribution of the protein layer on the titanium surfaces was evaluated thanks to two different techniques: surface potential imaging with Kelvin probe force microscopy (KPFM) and fluorescent microscopy.

Amplitude modulation KPFM was employed to obtain surface topography and surface potential simultaneously. This is a dual-scan system where the forward scan is performed in standard tapping mode, resulting in the topographical image, while the second scan is performed in lift mode applying a bias to the tip, allowing to obtain the surface potential image. The atomic force microscope (Innova atomic force microscope, Bruker) was equipped with a conductive tip (Sb-doped Si, frequency 75 kHz, SCM-PIT-V2, Bruker). Images (100 × 100 µm) were acquired at the border of the area where proteins were adsorbed. Gwyddion free software [40] was used for data manipulation.

Fluorescent microscopy was performed on the samples by using the optical profilometer in microscope mode (emission wavelength: 540–562 nm).

The scope of this analysis was to observe the coverage of the surface, not to quantify or compare the signal intensity among different samples, which was done as previously described, therefore color gamma has been post-processed in order to obtain the best visual results. No fluorescent signal has been detected on the titanium surfaces without adsorbed proteins.

2.8. Zeta potential measurement

ζ potential vs pH curves were obtained for protein in solution, as prepared surfaces and adsorbed samples. The potential of BSA and FN was measured via dynamic light scattering (DLS) (Litesizer 500, Anton Paar, Gratz, Austria): proteins were dissolved in PBS with an initial concentration of 35 and 0.2 mg/ml for albumin and fibronectin respectively. A further dilution in KCl 1 mM electrolyte was used to reach the final concentration of 5 mg/ml for BSA and 0.01 mg/ml for FN [41]. The protein potential was measured at different pH (2.5, 3, 3.5, 4, 5, 6, 7, 8, 9) by manually titrating the solutions with NaOH and HCl.

Solid surface ζ potential was measured with an electrokinetic analyzer (SurPASS, Anton Paar, Gratz, Austria) equipped with an automatic titration unit. A pair of samples were mounted on an adjustable gap cell and the curve was obtained by performing the acid and basic titration range separately. As for protein in solution, the electrolyte was KCl 1 mM and NaOH and HCl 0.05 M were used for titration; 15 pH points were considered for each range. A new pair of samples was measured for acid and basic titration, to avoid possible artifacts due to surface modification at extreme pH [41].

2.9. Attenuated total reflectance (ATR) infrared spectroscopy

Fourier transform infrared (FTIR) spectroscopy was performed in ATR mode with an FTIR spectrometer (Nicolet iN10 Infrared Microscope, Thermo Fischer Scientific, Waltham, USA) equipped with a Se/Ge ATR tip. Spectra were collected in the range 700–4000 cm^{-1} with the MCT detector, previously cooled with liquid nitrogen. 64 scans with a resolution of 4 cm^{-1} were used for each spectrum. Prior to each measurement, the air spectral background was collected with the tip in the air. Three different spectra were collected for each sample and averaged before plotting. Deconvolution of the Amide I band was performed with the dedicated tool in the OMNIC software, Thermo Scientific Peake Resolve, using the Savitsky-Golay second derivative method for the minima identification, adopting a Voigt function for the peak shape. A linear function was employed for the baseline correction.

3. Results and discussion

3.1. Surface properties

Protein adsorption at the interface with biomaterials cannot be understood and discussed without a deep knowledge of the properties of the surface itself. This research builds on previous investigations of surface chemistry, morphology and bioactivity of the surfaces employed in this work [30,35,41,42]. Herein, a characterization of the surface features specifically involved in protein adsorption has been carried out such as surface topography, surface composition and hydroxylation, wettability, surface energy, and surface potential.

At first, the topographical parameters (Table 1**)** and the 3D reconstruction of the investigated surfaces were calculated from laser confocal microscopy measurements (Fig. 1 a-c). As a reference, two samples representing the surface before the chemical treatment are considered: a mirror polished one (Ti64) and a grinded one (Ti64#400). After the chemical treatments, the samples have higher roughness than the reference samples and significantly different values from each other, both considering the average roughness (S_a) and the root mean square roughness (S_q): Ti(A-HC-H) is the roughest and Ti64(HF-H_2O_2) the flattest. These results are in agreement with the qualitative observations reported in previous works: Ti(A-HC-H) and Ti64(SrAg) have an oxide layer composed of oxide filaments and deep and elongated (along the Z axis) pores, while Ti64(HF-H_2O_2) has a more compact and thin surface layer, in the form of a nanosponge, with much smaller, less deep, and circular pores [35,43]. All the investigated surface treatments are developed for osseointegration and these roughness values are well suited for osteoblast adhesion and proliferation [44].

S_a and S_q values are widely used alone to quantify the roughness, but they are not enough for a comprehensive characterization of the shape of the surface features: the S_q/S_a ratio, skewness (S_{sk}) and Kurtosis (S_{ku}) are of interest at this purpose. An S_{sk} value below 0 corresponds to a profile with more valleys than peaks, while, on the other hand, a positive value of skewness is related to a higher distribution of features above the surface average plane. It is of interest that Ti(A-HC-H) has a positive value of S_{sk} differently for all the other surfaces and protruding areas are evident in the 3D reconstruction of the surface (Fig. 1 **a**). These data are also confirmed by the probability density function (PDF) and the Abbot-

Table 1
Topographical parameters (average ± standard deviations) of the investigated surfaces before protein adsorption.

	Ti64	Ti64 #400	Ti(A-HC-H)	Ti64(SrAg)	Ti64(F-H_2O_2)
S_q (μm)	0.05 ± 0.01	0.22 ± 0.04	0.96 ± 0.21	0.48 ± 0.10	0.25 ± 0.03
S_a (μm)	0.04 ± 0.01	0.17 ± 0.03	0.77 ± 0.18	0.36 ± 0.08	0.12 ± 0.02
S_{sk}	−0.49 ± 0.27	−0.79 ± 0.28	0.51 ± 0.09	−0.83 ± 0.12	−0.56 ± 0.22
S_{ku}	3.16 ± 0.46	4.61 ± 0.89	3.236 ± 0.141	5.356 ± 0.387	5.646 ± 2.865
S_q/S_a	1.26 ± 0.01	1.29 ± 0.05	1.26 ± 0.02	1.35 ± 0.05	1.28 ± 0.03
A_s/A_p	1.000 ± 0.000	1.003 ± 0.001	1.009 ± 0.002	1.010 ± 0.002	1.006 ± 0.002

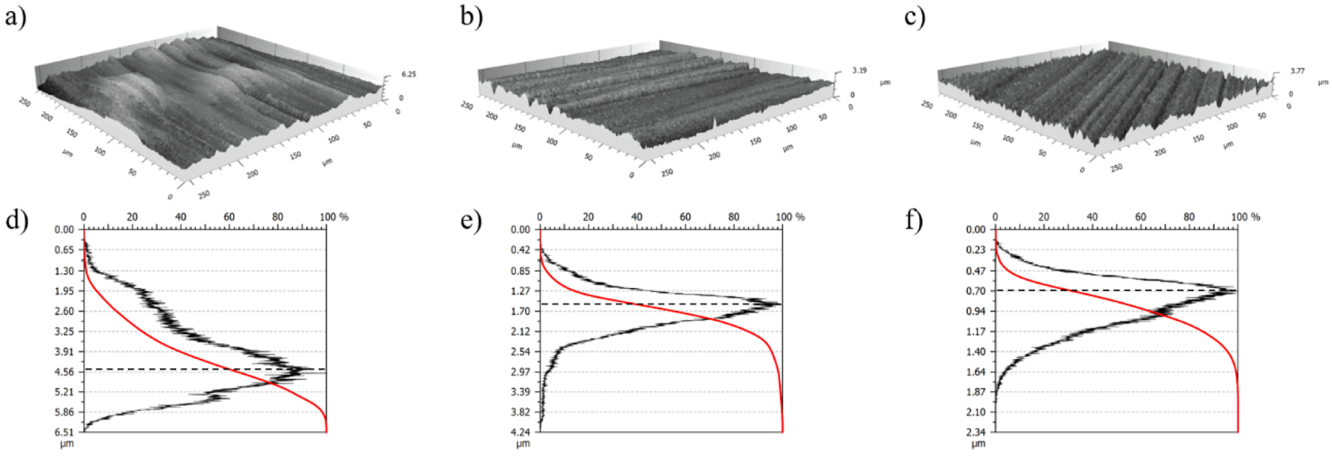

Fig. 1. 3D reconstruction images of titanium surfaces (a-c) and graphs showing the corresponding probability density function (black line) and Abbot-Firestone curve (red line)(d-e), the abscissa 0 is set at the highest point of the surface and the axis is directed downward, inside the surface: a,d) Ti(A-HC-H); b,e) Ti64(SrAg); c,f) Ti64 (HF-H_2O_2). The dashed lines represent the average line of the surfaces.

Firestone curve, which is the cumulative amplitude density function (Fig. 1 **d-f**). In all cases, the PDFs are slightly asymmetrical, showing tails towards the values lower than the average line of the surface for Ti64 (SrAg), and Ti64(HF-H_2O_2), as in the case of surfaces with a predominance of valleys, and a tail above the average line for Ti(A-HC-H).

Sq/Sa and Sku are correlated, and both refer to the shape of the top or bottom of the surface features: sharp features are expected if Sku and Sq/Sa are larger than 3 and 1.25, respectively, which are the reference values for a Gaussian height distribution. This is the case of Ti64(SrAg), which is significantly different from all the other surfaces for both the considered parameters (with low standard variation).

Comparing the surface area (A_s), which corresponds to the real surface area of the samples (while the projected area (A_p) is the geometrical area of the measured region), all the treated surfaces show a similar and a very limited increase of the real surface area with respect to the reference samples. This is slightly higher, as expected, in the case of Ti64 (SrAg) and Ti(A-HC-H).

In conclusion, the topography of the investigated surfaces can be summarized as follows: all the surface treatments induce an increment of roughness and surface area, which is larger for Ti64(SrAg) and Ti(A-HC-H). Ti(A-HC-H) has some features standing out; this is not surprising considering that this surface is affected by some fragility and occasional delamination phenomena [45]. Ti64(SrAg) has deep and sharp pores. Ti64(HF-H_2O_2) has the lowest roughness and depth of the pores. These data will be useful for understanding the differences in the amount of the adsorbed proteins because adsorption can be larger on rough surfaces offering more anchoring sites to the proteins [13].

The surface composition, obtained through XPS, for the various surfaces is reported in **Table S1** (see Supporting Information). All the samples show the expected chemical composition, along with some adventitious environmental contaminations [46], with a surface titanium oxide layer and the presence of Ca, Ag, and Sr ions on the surface of Ti64(SrAg). The degree of hydroxylation has been investigated through profile fitting of the oxygen region. The results are reported in Table 2 and Fig. 2.

Table 2
Binding energies and composition of the deconvoluted XPS peaks in the O1s region for titanium samples. The theoretical energies for each component are reported (-: non detected).

O1s Binding energy (eV)				
	TiO (529.8)	OHa (530.7)	OHb (531.6)	CO (532.3)/H_2O (532.8)
Ti	530.2	–	531.6	532.4
Ti64	530.1	–	531.3	532.3
Ti(A-HC-H)	529.8	530.8	531.6	532.4
Ti64(SrAg)	530.2	530.7	531.3	532.5
Ti64(HF-H_2O_2)	530.1	530.7	532.0	532.7 (H_2O)
Peak composition (%)				
	TiO	OHa	OHb	CO /H_2O
Ti	53.0	–	32.6	14.4
Ti64	61.3	–	26.3	12.4
Ti(A-HC-H)	81.3	5.9	8.6	4.2
Ti64(SrAg)	66.8	10.8	17.8	4.6
Ti64(HF-H_2O_2)	9.69	26.7	15.4	48.3 (H_2O)

Contributions from the Ti-O bond, OH groups, and adventitious carbon or adsorbed water (on Ti64(HF- H_2O_2) were found on all the surfaces. It can be observed that Ti and Ti64 have about 30% of the surface oxygen ions involved in OH groups and they have a basic behaviour (OHb), while the treated surfaces have between 19% and 42% of them. OH groups with an acidic behaviour (OHa) are absent on the untreated substrates and increase moving from Ti(A-HC-H), Ti64(SrAg), and Ti64(HF HF- H_2O_2) [39,47,48].

The measured water contact angles (θ) of the investigated surfaces are presented in Table 3. The surface treatments increase the wettability of the titanium surfaces, even though the difference between Ti(A-HC-H) and its control is not statistically significant. In particular, the lowest θ are observed for Ti64(HF-H_2O_2) and Ti64(SrAg).

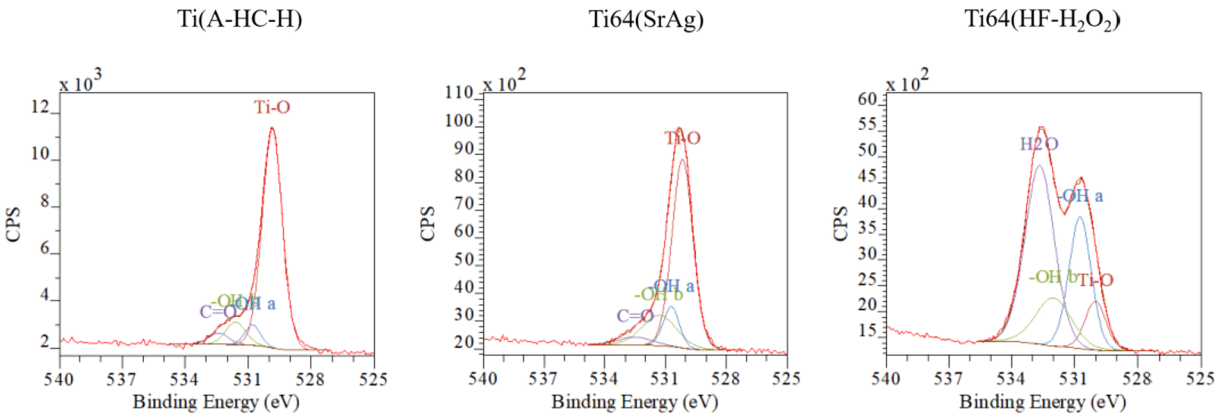

Fig. 2. Deconvolution of the O1s region for the treated titanium samples.

Table 3
Static water contact angle for the untreated and treated titanium surfaces.

Sample	θ (±St.Dev)(°)
Ti	49.2 ± 4.4
Ti64	53.5 ± 3.0
Ti(A-HC-H)	44.2 ± 2.8
Ti64(SrAg)	7.4 ± 0.4
Ti64(HF-H_2O_2)	28.4 ± 4.8

The results of the surface energy measurements are reported in Fig. 3-**a**. As expected from contact angle data, the untreated surfaces have the lowest values while the surface treatments increment the SFE, which is the sum of the polar (γ^p) and dispersive (γ^d) components. Ti64 (SrAg) shows the highest total surface free energy, followed by Ti64(HF-H_2O_2). A significant increment with respect to the control surfaces was not observed for Ti(A-HC-H). Interestingly, the dispersive component of the surface energy, which is due to temporary variations of the charge distribution in the molecules, is the same for all surfaces, while the polar one varies. Since γ^p is due to the functional polar groups or charged ions on the sample surface, the increase in the hydroxylation of Ti64 samples due to hydrogen peroxide treatment and especially to the incorporation of Sr^{2+} and Ag^{+} ions in the oxide layer is expected to increase the polar part of the surface energy. The trend of the polar component of SFE is correlated to that of wettability and it has been previously reported [49].

The various treatments strongly change the surface zeta potential (Fig. 3-**b**) and exposed functional groups, as has been deeply discussed in another work [35]. Ti and Ti64 have their isoelectric point (IEPs), which is the pH value that corresponds an overall zero charge of the surface, at 4.1 as expected for titanium and all surfaces without surface functional groups with a strong acid-basic reactivity [50]. In agreement with IEPs, both curves are characterized by the absence of evident plateaus, related to the absence of deprotonated/protonated functional groups affecting the surface zeta potential. We can conclude that, even if basic OH groups are present on these surfaces (see Table 2), they are not protonated in the explored pH range and they have a weak acid-basic reactivity. After treatments, all the surfaces have very different IEP and curve shapes than the untreated surfaces (Fig. 3-**b**). The acid-alkali treatment Ti(A-HC-H) results in a more positive surface, shifting the IEP to a higher value (5.6). The plateau in the acidic range suggests the presence of basic OH groups on the surfaces, which are fully protonated at a pH lower than 3.5, as expected for anatase surfaces [29]. Contrary, both Ti64(SrAg) and Ti64(HF-H_2O_2) have a very low IEP, respectively at 2.9 and 2.6 (deduced by interpolation), and a very clear plateau in the basic range, with similar onset at around 4.5. On those surfaces, the OH groups have a strong acidic behavior and they deprotonate completely at quite a low pH.

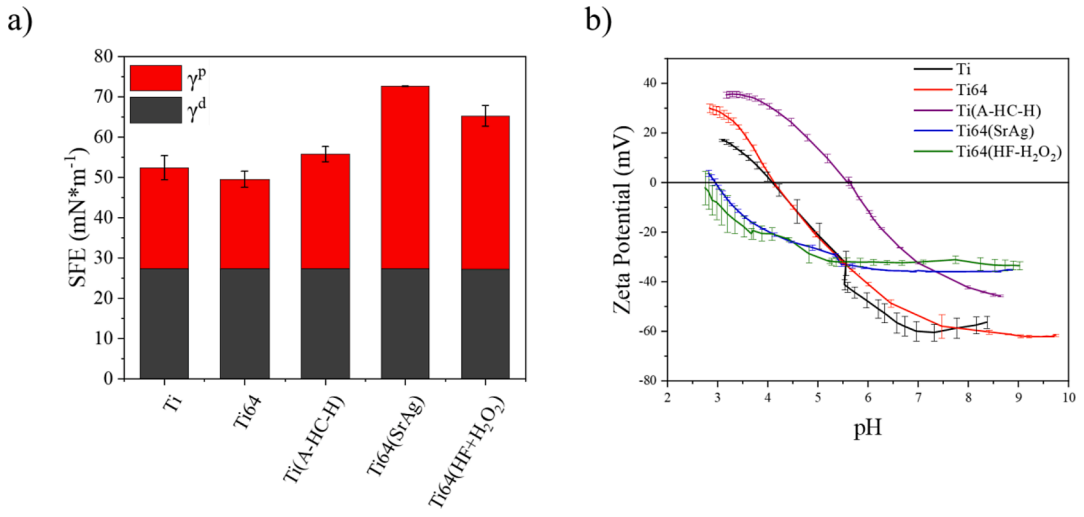

Fig. 3. a) total surface free energy of the different surfaces (whole bars) and their respective dispersive (dark grey bars)) and polar components (red bars); b) zeta potential titration curves of the samples.

3.2. Effect of surface treatments on the affinity for albumin and fibronectin

The amount of albumin and fibronectin adsorbed on the different surfaces was measured because it is among the main parameters that can control the interactions of titanium surfaces with cells [6]. Enhanced adsorption of the proteins with antiadhesive properties, such as albumin, is generally reported to hinder osteoblast, macrophages, and bacteria adhesion/proliferation resulting in a larger anti-inflammatory response and lower risk of infection, but lower osseo-induction ability, too [51]. On the other side, fibronectin is recognized as an adhesive non-collagenous glycoprotein resulting in faster osseointegration. A proper ratio between the adsorption of these two proteins is needed for surfaces able to induce osseointegration and with anti-inflammatory properties, to avoid chronic inflammation and fibrotic encapsulation of the implant.

The presence of an adsorbed layer of albumin and fibronectin on all the surfaces was confirmed by XPS chemical analysis (**Table S2** in Supporting Information). Nitrogen is a typical element of proteins and its increase is reported as a marker for protein adsorption [52,53]. According to Foster et al. [54], 9% of nitrogen corresponds to a complete surface coverage of the examined area. The atomic nitrogen is above such threshold for all the samples but Ti(A-HC-H)_BSA (**Table S2**), therefore, it is possible to hypothesize that proteins form a continuous layer on such surfaces. On Ti(A-HC-H)_BSA, the N% is a bit lower than the threshold value, but this can be related to local delamination of the oxide layer, as already described, reducing the amount of protein on the surface of this specimen. The other characterization techniques will confirm the formation of a continuous protein layer, also on this type of surface, by analyzing a larger area of the surface.

In this work, albumin and fibronectin adsorbed on the surfaces were quantified with two different techniques. Bicinchoninic acid protein assay is a well-established method to evaluate the concentration of proteins in a solution and it is widely employed for evaluating the amount of adsorbed proteins on titanium biomaterial surfaces, after they have been detached [19,55,56]; the results are shown in Fig. 4-**a**. All the chemical treatments are able to enhance the adsorption of albumin, with a statistically significative difference with respect to the controls. According to these data, the treated surfaces were found to adsorb a similar amount of proteins, in a range from 2.65 to 3.3 μg/cm^2.

The use of fluorescently labeled proteins allows a qualitative analysis of the number of proteins adsorbed, through direct optical detection of the fluorescent signal on the sample surfaces. The treated surfaces show again a much higher affinity for proteins with respect to the mirror polished controls and, according to these data, clear differences can be appreciated also between the different treatments, both for albumin and fibronectin (Fig. 4-**b**). Ti(A-HC-H) and Ti64(SrAg) can adsorb a bigger amount of albumin and fibronectin with respect to Ti64(HF-H_2O_2), with a larger difference in the case of BSA. The difference between the Ti(A-HC-H) and Ti64(SrAg) is also significant.

By comparing the results obtained with the two analytical methods, it is possible to hypothesize a limitation in the BCA protein assay for the investigation of albumin adsorption on biomaterials. It has been already acknowledged that sodium-dodecyl sulfate (SDS) cannot remove all the proteins from a surface[57] with different efficiency according to the particular investigated protein. Since only the detached proteins are detected by the BCA protein assay, different removal efficiency by the SDS, which can be related to protein-surface interaction strength, will lead to an underestimation of the adsorbed proteins and an incorrect comparison between the surfaces. Here, the great differences in the comparison between samples observed in the albumin adsorption investigated by BCA or fluorescent proteins may be related to a very limited detachment of proteins from the pores, mainly on Ti(A-HC-H) and Ti64(SrAg) samples, and to different binding strength. It is therefore necessary to carefully consider whether the BCA protein assay is a suitable technique for providing quantitative results on the protein adsorption on structured surfaces for biomedical applications.

The enhanced adsorption of proteins on the treated surfaces may arise from different factors. It is reported in the literature that the micro- and nano-structures of the surfaces increase the available protein binding sites [13] and pores can act as physical traps for proteins [58]. On one side, surface hydrophilicity is generally regarded as a limitation for protein adsorption, on titanium biosurfaces, as well as on other materials [59,60]. On the other side, an increase in wettability can avoid a Cassie-Baxter regime, stimulating surface-solution contact within the pores. A higher SFE, in particular the polar component, was found to promote protein-surface interactions [61]. In the surfaces investigated in this work, there is a concomitance of factors. All the treated samples have both higher roughness and porosity and γ^p with respect to the untreated controls, accounting for the great increase in the adsorption. Even though Ti64(HF-H_2O_2) has higher SFE than Ti(A-HC-H), close to the one of Ti64(SrAg), it adsorbs much fewer proteins, in particular looking at the fluorescence data. It can be concluded that the morphological effect overcomes the chemical one in determining the amount of adsorbed proteins on titanium surfaces. It must be considered that the difference in the exposed surface area among the treated surfaces is not so high to explain the different adsorption: it means that the shape of the porosity has a role and the deeper pores on Ti(A-HC-H) and Ti64(SrAg) can physically entrap more proteins than the compact porosity of the Ti64(HF-H_2O_2). When the pore structure is similar, as in the case of Ti (A-HC-H) and Ti64(SrAg), the latter is the one adsorbing more, thanks to the sharp shape of the pores. The higher surface energy, and presence of silver and strontium, which are known to have a strong affinity for proteins [62,63], can play a second order role. The surface morphological effect is greater when albumin is involved in adsorption instead

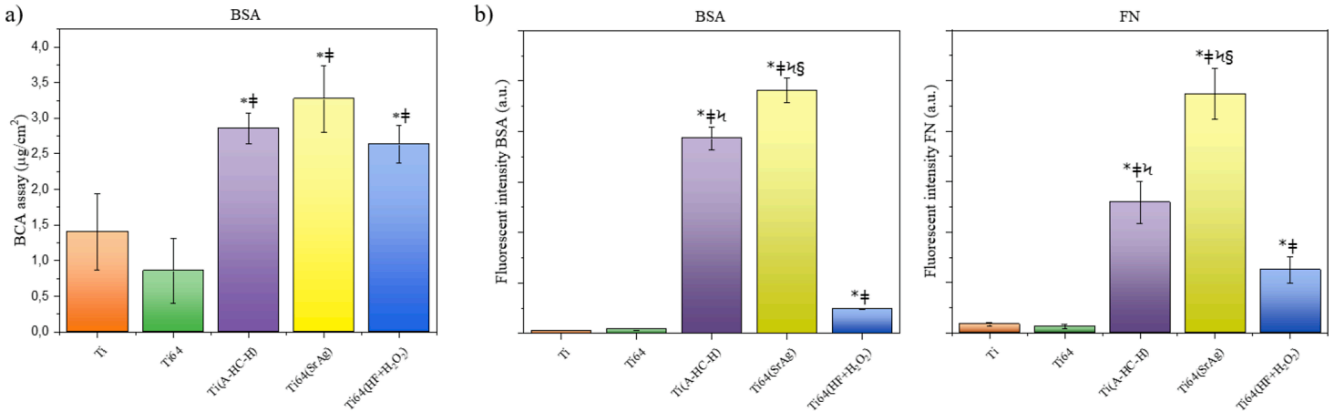

Fig. 4. a) Albumin (bovine serum albumin, BSA) quantification by BCA protein assay; b) BSA and fibronectin (FN) quantification by fluorescent-conjugated proteins. Statistical significance was set at a $p < 0.05$: * vs Ti; ‡ vs Ti64; vs Ti64(HF-H_2O_2); § vs Ti(a-HC-H).

of fibronectin due to their different dimension: fibronectin is much larger than albumin and it can penetrate less within the pores. As an effect, Ti64(HF-H_2O_2) has a larger difference in the amount of adsorbed albumin, but a lower one concerning fibronectin when compared to the other treated surfaces.

3.3. Surface coverage and imaging of the protein adsorbed layer

Cell-biomaterial interactions are mediated by the transient protein matrix, where it forms. So, the distribution of the protein layer on the surface is fundamental to understanding the biomaterial biological response. The results of the fluorescent imaging are shown in Fig. 5. No autofluorescence was observed for titanium substrates without proteins (images not shown).

On all the surfaces, both albumin and fibronectin form a continuous layer. On Ti64(SrAg) and, to a lesser extent, on Ti(A-HC-H) there seems to be an accumulation of proteins within the grooves. This can confirm the effect of the surface topography on protein adsorption. The adsorption on Ti64(HF-H_2O_2) seems more homogeneous, possibly due to the lower roughness and absence of very deep valleys. Looking at the fibronectin adsorbed onto Ti(A-HC-H) it is possible to notice some black areas, where there are no or very few adsorbed proteins. As already explained, the oxide layer on this surface can occasionally delaminate: on those points, the adsorption is extremely lower, confirming the extreme increase of protein-surface interactions where the chemical treatment has been effective.

The extent of the protein layer was also observed at larger magnification, thanks to the use of KPFM. The topographical and surface potential images after albumin adsorption on a limited area of the sample surface are reported in Fig. 6.

On each substrate, the adsorbed protein layer is not observable in the topographical images, while it is revealed in the surface potential ones. The areas exposed to albumin show a lower potential (darker color) compared to the clean surfaces (yellowish). As already reported in the literature, biomolecules, such as DNA, have a lower potential than biosurfaces [64,65], and this was observed specifically for albumin on Ti6Al4V alloy by Rahimi et al. [66] and by the authors in previous work [67]. Thanks to this technique, it is possible to observe the protein layer at much higher magnification with respect to fluorescent microscopy, allowing to assess the homogeneity and continuous coverage of the protein layer on all the surfaces, in particular on Ti(A-HC-H) and Ti64 (HF-H_2O_2). On Ti64(SrAg) the potential of the adsorbed proteins is a little less homogeneous, possibly depending on the intrinsic variation in the surface potential of the substrates (here not shown). Still, it is possible to see the accumulation of proteins within the grooves, such as the one almost in the center of the image, which is very dark, confirming the effect of topographical features in the adsorption process. The variation in the differences between the surface potential of the specimens and the one of the adsorbed BSA, which is about 150 mV for Ti(A-HC-H), 15 20 mV for Ti64(SrAg) and 50 mV for Ti64(HF-H_2O_2), may be due to a different work function of the substrates themselves, that change up to some volts, [68] or to a different orientation of the proteins on the surface.

The KPFM images obtained for fibronectin adsorption on a limited area of the samples are reported in Fig. 7. They are very similar to the ones obtained for albumin adsorption. Also with fibronectin, a continuous protein layer is formed on all the substrates and it can be detected only in the potential images. The potential differences between the three titanium surfaces and the FN adsorbed layer are 70 mV, 25 mV and 80 mV for Ti(A-HC-H), Ti64(SrAg) and Ti64(HF-H_2O_2), respectively.

The fact that the protein layer is not observable in the topographical images correlates with the hypothesis that protein adsorption occurs in a monolayer or very few molecular layers, with a thickness of few nanometers [69,70]. Furthermore, the fact that the topographical features are not hidden by the transient protein matrix is beneficial for the osteointegration of the surfaces: after the formation of the protein layer, osteoblasts will still be able to sense the surface roughness, which can stimulate their adhesion and activity [71].

3.4. Protein orientation and conformation after adsorption

The biological activity of proteins is closely dependent on their 3D structures, both secondary and tertiary. For example, a change in the protein chain folding can deactivate enzymes [72] or fibronectin can expose cell binding RGD sequences upon denaturation [73,74]. Also, according to the orientation of the protein on the sample, different areas of the protein surface may be turned outward, with the exposition to the environment of hydrophilic/hydrophobic patches or positive/negative residues [11].

The chemistry of the adsorbed proteins was investigated by deconvolution of the C1s and N1s XPS peaks (Table 3S and Fig. 1S in Supporting Information) and the measurements confirm that both albumin

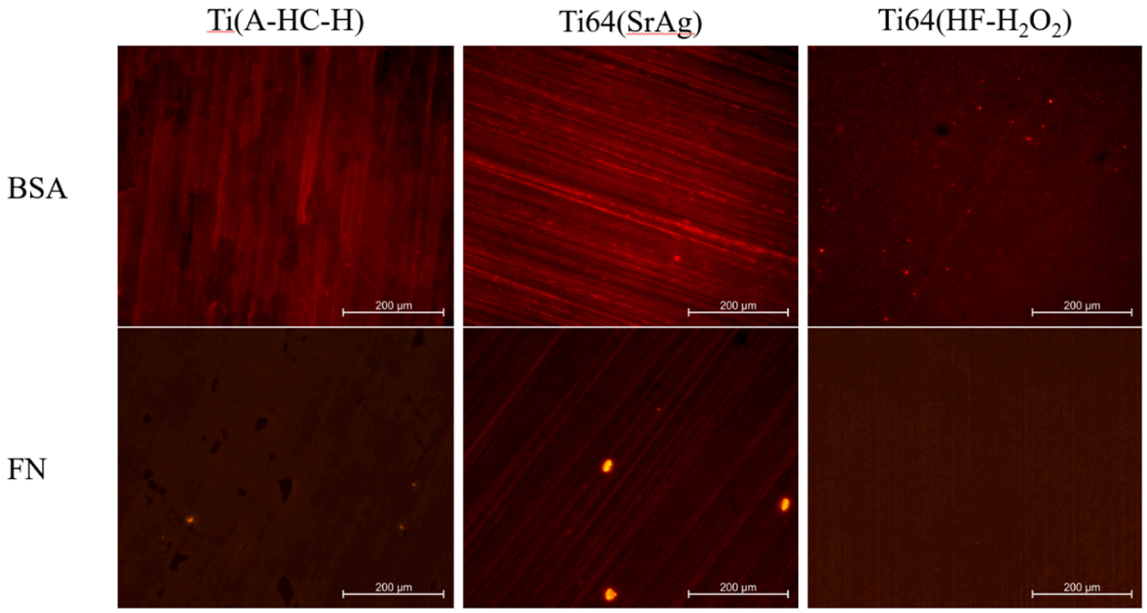

Fig. 5. Fluorescent images of rhodamine-conjugated albumin and fibronectin adsorbed on the different surfaces (200x).

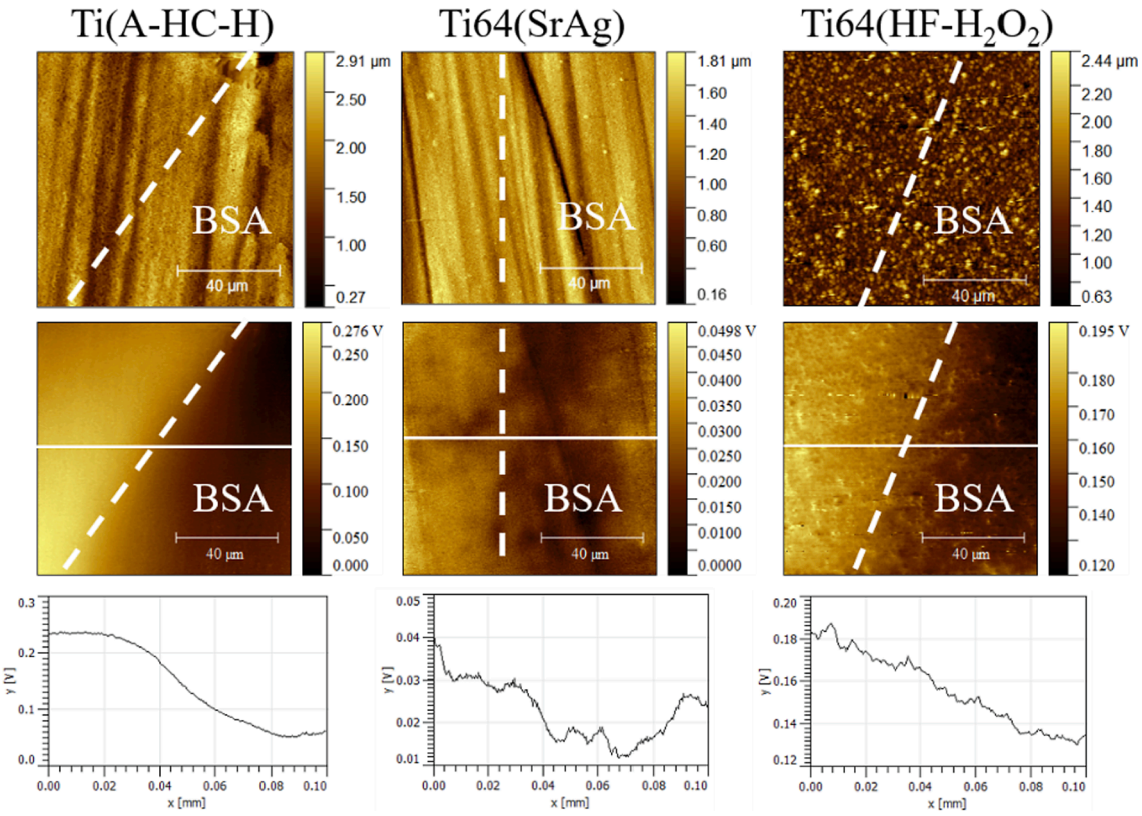

Fig. 6. KPFM images of samples after albumin adsorption on a portion of the surface: topographical image (first row); surface potential image (second row); potential profile along the white line (third row). Dashed lines separate areas without (left of the line) and with (right of the line) albumin layer.

and fibronectin are chemically un-modified after adsorption, with any rupture or formation of covalent bonds. It is also confirmed that they adsorb in their charged form, with both negative COO^- and positive NH_3^+ groups present on the surface. Those groups may have an active role in the adsorption process, in particular by forming hydrogen bonds or electrostatic interactions with the hydroxyl groups of the titanium surfaces [16,75].

Being very sensitive to a wide range of surface modifications, the zeta potential may provide interesting information about the charge and hydrophilicity characteristics of the surfaces, before and after protein adsorption. Similarity among titration curves means that similar functional groups are exposed on the surfaces. When there is an adsorbed protein layer, this shows that proteins have the same orientation or three-dimensional conformation (tertiary structure) upon adsorption. Eventual changes in the protein structure adsorbed on titanium substrates will also result in titration curves different with respect to the ones of the native protein in solutions.

To be sure of the real meaning of the titration curves on the surfaces upon adsorption, it was verified if the adsorbed protein layer was eventually removed during the titration measurements. This is also of biological interest because the higher the residual protein after the acid titration, the stronger are the protein surface interactions, even if the pH goes down as it occurs during inflammation (pH 4.0–4.5). The amount of nitrogen detected on the surface by XPS after the acid titration has been used for this purpose. Both on Ti_BSA and Ti64_BSA, the amount of residual N after the acidic titration (Table 4) is sensibly less than the one found just after adsorption (**Table S2** in Supporting Information), as a consequence of protein detachment during the titration. During an electrokinetic zeta potential measurement, reactions or modifications of the surfaces can determine instability of the potential values and, as consequence, high standard deviations [35]. Therefore, the pH at which proteins begin to detach from the surface can be found where the standard deviation increases. In the case of Ti_BSA and Ti64_BSA, the deviations are low (<5 mV) for most of the measurements, spiking up to values greater than 10–15 mV at pH equal to or lower than 4. Instead, on all the treated surfaces, the nitrogen amount is comparable to the values obtained just after albumin adsorption, signaling that the protein is not washed away. In fact, for these samples the standard deviations are always low (<5 mV) along with all the titration measures. This means that the interactions between albumin and the chemically modified surfaces are strong and stable enough not to be disrupted by the electrolyte flow or the pH titration.

IEP of Ti(A_HC-H) with FN is not significant and not reported.

After fibronectin adsorption, the samples mostly behave in the same way. On Ti_FN and Ti64_FN both the N% and the standard deviations along the titration indicate a detachment of the proteins around pH 4, while on Ti64(SrAg)_FN and Ti64(HF-H_2O_2)_FN adsorbed fibronectin is not removed.

Protein detachment from the reference polished surfaces might be caused, among other factors, by the changes in the surface charges. In fact, below pH 4, both Ti and Ti64 surfaces are positively charged and the proteins lose their negative functional groups, since $-COO^-$ get protonated at about the same pH [76] exposing only the protonated amino residues. The absence of porosity on the untreated samples have also a role in weak adsorption. It is of biological interest that the adsorbed proteins are chemically instable and easily detached from Ti polished surfaces at pH close to the inflammatory response.

On the other hand, Ti64(SrAg) and Ti64(HF-H_2O_2) expose deprotonated hydroxyl groups in all the measured pH range (acting as a strong acid), being always capable of binding with the positive patches on the proteins even at inflammatory pH.

Ti(A-HC-H)_FN is an exception. In fact, the standard deviations on this curve are very low during the titration, but the final N% is greatly reduced with respect to before the zeta potential titration. It can be supposed that fibronectin is early detached from the surface even before the titration starts. The weak link of fibronectin to Ti(A-HC-H) is of

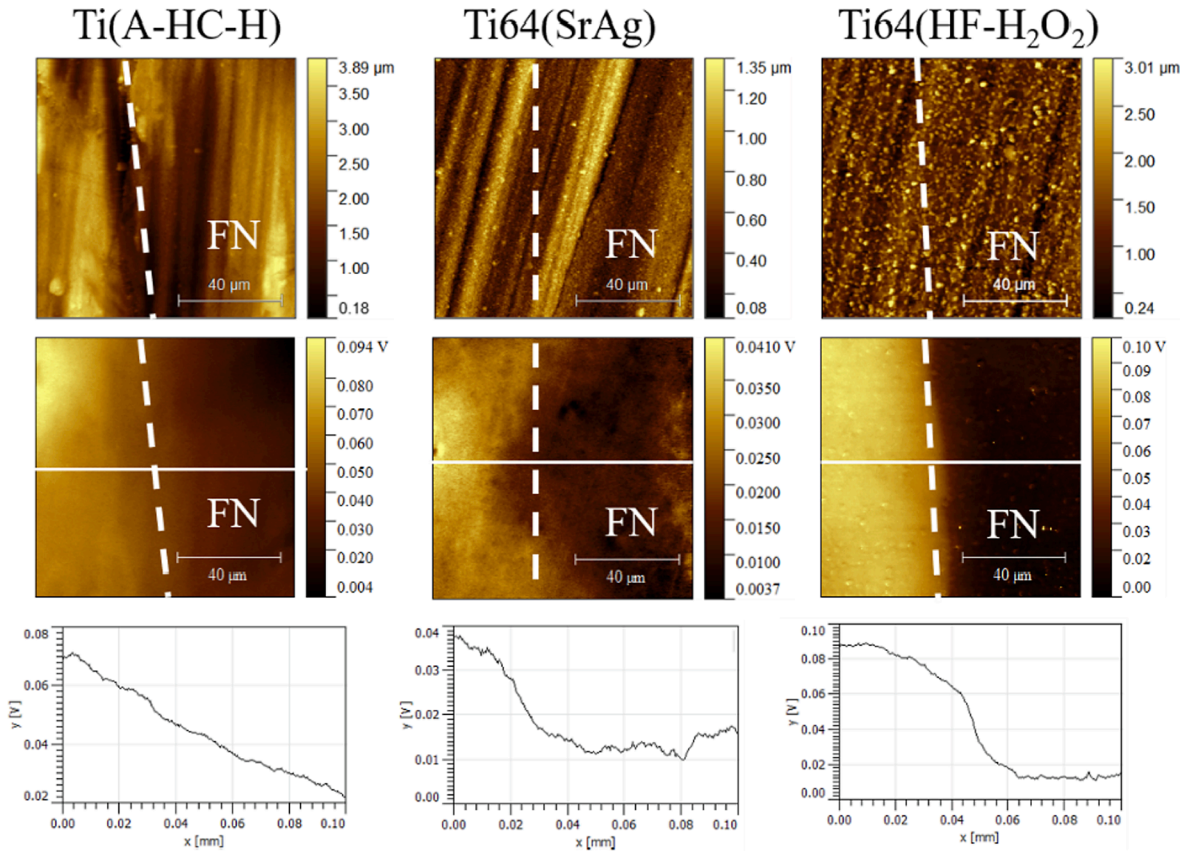

Fig. 7. KPFM images of samples after fibronectin adsorption on a portion of the surface: topographical image (first row); surface potential image (second row); potential profile along the white line (third row). Dashed lines separate areas without (left of the line) and with (right of the line) the fibronectin layer.

Table 4
IEPs of the surfaces as prepared (a.p.) and after adsorption of albumin and fibronectin. The nitrogen atomic percentage on the surfaces after the zeta potential titration in the acidic range (-, not applicable).

	IEP			N% residual	
	a.p.	**BSA**	**FN**	**BSA**	**FN**
Protein	–	4.5	4.9	–	–
Ti	4.1	5.0	4.6	8.43	8.11
Ti64	4.9	4.8	4.6	8.23	6.92
Ti(A-HC-H)	5.6	5.0	–	11.09	3.01
Ti64(SrAg)	2.9	4.6	4.4	10.67	13.12
Ti64(HF-H_2O_2)	2.6	4.5	4.3	12.93	11.68

biological interest. The high IEP of this surface and its positive charge at any pH lower than 5.5 can play a role in this phenomenon. Albumin is not removed during the potential measurement thanks to a more efficient entrapment inside the surface pores, due to its small dimension. A secondary effect can be due to the mechanical instability of the oxide layer of this surface, too [45,77]. Because of this result, the Ti(A-HC-H)_FN curve cannot be considered informative for the characterization of the adsorbed layer of fibronectin.

After albumin adsorption (Fig. 8-**a**) the potential titration curves are different compared to the bare substrates and protein in solution (Fig. 3-**b**). In particular, the IEPs of all the substrates are moved towards the one of BSA (Table 4), which is about 4.5 [78], confirming the presence of an adsorbed protein layer and mostly complete surface coverage.

The curves of Ti_BSA and Ti64_BSA are quite similar, meaning that albumin assumes a similar tertiary conformation and orientation on the untreated surfaces. With respect to the native protein, albumin adsorbed on Ti and Ti64 exposes more hydrophobic moieties outwards, since the linear segment of the curve around the IEP has a much higher slope [79].

In the same way, albumin adsorbed on Ti64(SrAg) and Ti64(HF-H_2O_2) has a very similar behavior of the zeta potential versus the pH, with the same IEP and same zeta potential at the plateau. The adsorption on these surfaces may lead to a similar 3D structure of the protein in the transient layer, which is also quite close to the tertiary structure of albumin in solution (hydrophilic moieties outwards). In the case of Ti(A-HC-H)_BSA, adsorbed albumin seems to be in a configuration that is almost in the middle between that the other treated surfaces and the untreated ones.

In the case of adsorbed fibronectin (Fig. 8-**b**), the presence of a protein layer is again confirmed due to the shift of the IEPs, the N residues (Table 4) and the changes in the shape of the titration curves, compared with the bare substrates and protein in solution (Fig. 3-**b**); as already explained, an exception is Ti(A-HC-H)_FN. The adsorbed fibronectin assumes a similar 3D configuration both on the untreated and treated surfaces. Ti_FN and Ti64_FN overlap almost perfectly and show more hydrophobic behavior with respect to native fibronectin, as it occurs for albumin. Ti64(SrAg)_FN and Ti64(HF-H_2O_2)_FN are slightly shifted with respect to the untreated surfaces, but they have a similar slope around the IEP. In the case of the adsorbed fibronectin, it can be assumed that its orientation and tertiary structure are not significantly changed by the type of the surface, probably because of the larger dimension of the protein, and it exposes in any case much more hydrophobic moieties than the native configuration, after adsorption.

Both Ti64(HF-H_2O_2)_BSA and Ti64(HF-H_2O_2)_FN show the onset of the plateau in the basic range at lower pH than the other samples, but it cannot be excluded that the underlying substrate and the thinner adsorbed layer have an effect on this behavior.

In conclusion, concerning the tertiary structure and orientation of the proteins: albumin adsorbed on treated surfaces is closer to the native proteins (more hydrophilic moieties outwards) than it is on the

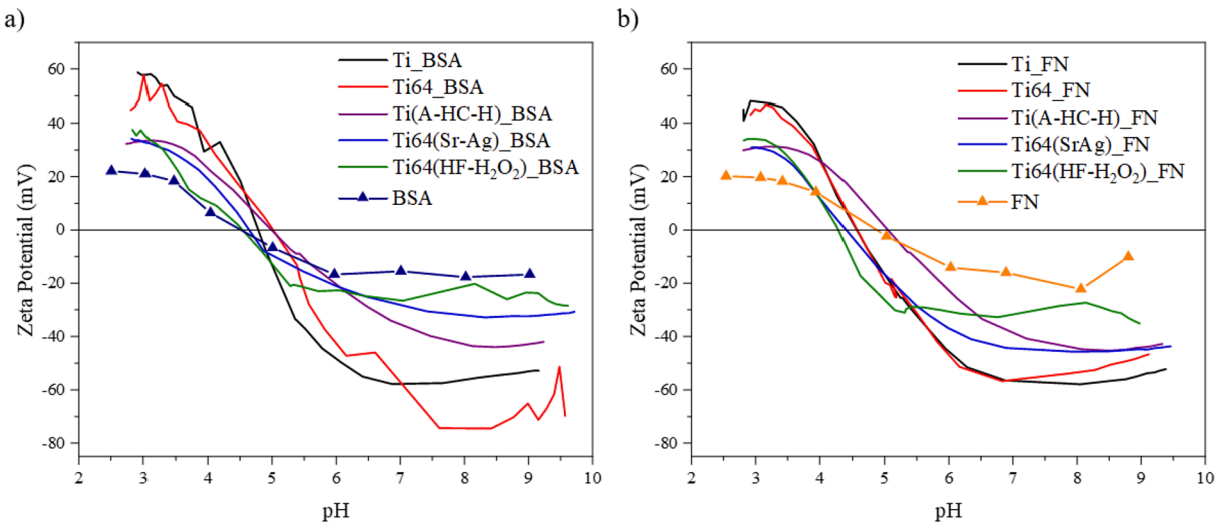

Fig. 8. Zeta potential titration curves of untreated and treated titanium surfaces after adsorption of albumin (a) and fibronectin (b). The curves of the respective proteins in solution are also reported.

untreated surfaces, while fibronectin has a similar tertiary structure on the treated and untreated surfaces with more hydrophobic moieties outwards than in the native state. Both proteins have a compact form when in solution, and albumin has been reported to maintain its overall structure, with hydrophobic domains inwards and hydrophilic domains outwards, when adsorbed on hydrophilic surfaces, while it tends to spread on hydrophobic ones [80], in agreement with the ζ potential results. As consequence, the main ligand binding sites of albumin I and II [32], contained in hydrophobic cavities in subdomains IIA and IIIA [81], are hidden from the surrounding environment. Contrary, fibronectin tends to assume a more elongated conformation on surfaces with higher wettability [82]. The change of fibronectin spatial organization after adsorption on the treated surfaces can be beneficial thanks to the exposure of the RGD well known adhesive sequence, that can be recognized by α5β1 integrins on the cell membrane and increase cell adhesion [83]. According to the results, it can be speculated that the tertiary structure of albumin is more strongly affected by the charge, wettability, polar component and SFE of a surface, which are similar for Ti64(SrAg) and Ti64(HF-H_2O_2), than by other surface features. On the other side, a big protein such as fibronectin is less affected by these surface characteristics.

The protein-surface interactions, along with entropy gain associated with the adsorption process, can alter the equilibrium of forces (hydrophobic, electrostatic, hydrogen and Van der Waals bonding) that maintain the 3D structures of the peptide backbone and secondary structure, such as α-helices and β-sheets [84]. It has been demonstrated that adsorption on different titanium surfaces can alter the secondary structure of albumin [55] and fibronectin [85], reducing or increasing the number of helices and sheets according to the amount and type of OH surface groups. A suitable characterization technique to investigate this aspect on adsorbed proteins is FTIR:

After adsorption of albumin and fibronectin, the FTIR spectra collected on all the modified surfaces show the typical protein adsorption bands, Amide I and Amide II, (Fig. 9). The Amide I band (≈1650 cm^{-1}) arises from the stretching vibration of C═O bonds and it is strictly dependent on the secondary structure of the protein, the Amide II band (≈1550 cm^{-1}) is due to a combination of the CN stretching vibration and the NH in plane bend, its correlation with the protein secondary structure is less obvious than for the Amide I.[86] As consequence, the Amide I band was deconvoluted in order to assess the effect of the surfaces on

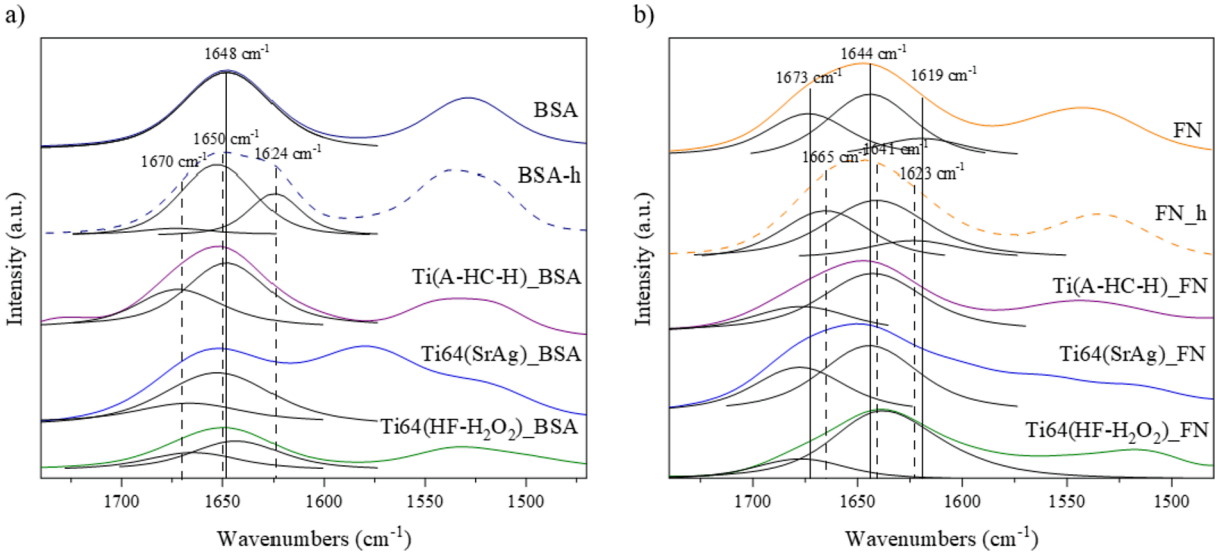

Fig. 9. Amide I and Amide II bands region of BSA (a) and FN (b), as native or denatured proteins and after adsorption on the different samples, with deconvolution of the Amide I band. The component positions of the native (solid lines) and denatured (dashed lines) proteins are also reported.

the conformation of adsorbed proteins. After adsorption of both proteins, Amide I and Amide II bands, which were absent prior to adsorption (**Figure S2**), were analyzed on each sample (Fig. 9).

In the albumin reference spectra (Fig. 9-**a**), Amide I band has a single component, at 1648 cm^{-1}, corresponding to the α-helix. After thermal denaturation, while the α-helix band remains unchanged, two contributions arose, one at lower wavenumber (at about 1624 cm^{-1}) that can be attributed to the formation of β-sheets, and a minor one (at about 1670 cm^{-1}), due to β-sheets or β-turns [87–89]. After adsorption on Ti (A-HC-H) and Ti64(SrAg), the contributions of α-helix and β-structures have been found, indicating a partial denaturation after adsorption, with a partial loss of the helical portion (Table 5). On Ti64(SrAg), a broad band around 1580 cm^{-1} was also detected and can be attributed to a signal from the substrate (**Figure S2-b**). A much stronger denaturation was observed on Ti64(HF-H_2O_2), where a shift of the main band was observed to values corresponding to unordered structures (1643 cm^{-1}) [86,90,91]. The quantitative evaluation of the loss of the α-helices, which derives from the calculation of the integrated areas of the deconvoluted components, should be considered with the due caution, particularly to the spectral resolution used for these analyses, which is nominally 5 cm^{-1} and to the eventual overlapping of minor signals of the substrate, as well as the deconvolution method itself, could influence the fine positioning of the single fitted components. However, the reliability of the obtained results is supported by literature and by the coherence of these findings with knowledge provided by the other measurements carried out in this study.

Regarding fibronectin (Fig. 9-**b**), the native and denatured proteins show contributions corresponding to random coils at 1644–1641 cm^{-1}, β-sheets at 1619 and 1623 cm^{-1}, and β-sheets/β-turns at 1673 cm^{-1} and 1665 $cm^{-1}$for FN and FN_h, respectively. The denaturation provokes a small band shift and a reduction of the random coils, while the β-sheets or β-turns structures increase (Table 5). Still, as already discussed for BSA adsorption, the accurate quantitative evaluation of the contribution of random coils and β-sheets is calculated through the relative evaluation of the measured samples, being conscious of the practical difficulties related to the strict determination of the number of components of a band and their actual frequency upon deconvolution of strongly overlapped peaks. However, the obtained results show that fibronectin adsorbed on Ti(A-HC-H) and Ti64(SrAg) has a similar loss of the β-sheet structure (Table 5), in favour of the formation of random coils and β-turns. On the other hand, FN shows a very broad contribution at 1639 cm^{-1} on Ti64(HF-H_2O_2), which here was namely attributed to β-sheets.

In conclusion, when proteins adsorb on the titanium treated surfaces, denaturation occurs in the case of both albumin and fibronectin, with different characteristics on each surface. On Ti(A-HC-H) and Ti64(SrAg) the proteins adopt a similar conformation, while on Ti64(HF-H_2O_2) the results are quite different. Albumin and fibronectin almost retain their native structure on the former two surfaces, while it is more disrupted on the latter. Secondary structures of adsorbed proteins, albumin in particular, have been found in the literature related to the surface chemistry of titanium substrates: a high surface hydroxylation is related to a loss of α-helices, while negatively charged surfaces may promote β-sheet structures [55]. Our data agree with this hypothesis and they allow us to take a step forward. Ti64(HF-H_2O_2) has a high amount of strong acidic OH groups, which are in the Ti-O^- state at the pH of adsorption, and this can explain the high content of random coils and β-sheets that compose adsorbed albumin and fibronectin, respectively. On the other hand, the presence of acidic OH groups is not the only determining factor for protein denaturation. Ti(A-HC-H) and Ti64(SrAg) have both acidic OH, in different concentrations with respect to one another, still proteins adsorbed on them have a similar structure, less denatured than on Ti64(HF-H_2O_2). It seems that there is a threshold in the concentration of total and acidic OH below which the protein-surface interactions are not enough to disrupt the protein secondary structures. Changes in the protein secondary structure after adsorption are reported to have an impact on cell adhesion and spreading on the materials. Recently, a decrease in the α-helical content has been reported as beneficial for stromal cell adhesion [92], and a pro-adhesive behavior of the albumin layer has been also reported in the case of macrophages and platelets [93]. As well as fibronectin spreading on the surface after adsorption, the changes in its secondary structure can contribute to revealing the RGD tripeptide for cell recognition and binding. Thus, the different conformation of adsorbed albumin and fibronectin, in particular on Ti64(HF-H_2O_2), can affect the response of relevant cells such as macrophages, fibroblasts and osteoblasts. Indeed, the results presented in this paper are in line with previous studies where the biological activity of the different treatments has been studied separately. Ti(A-HC-H) has superior bone bonding ability, in terms of bone maturation and detachment load, than untreated pure titanium [94]. Besides the increased bioactivity (precipitation of hydroxylapatite) of the treated surface, higher adsorption of pro-adhesive proteins than the untreated Ti surface can improve surface colonization by osteoprogenitor cells. Ti64(SrAg), despite the assessed antibacterial property, has no cytotoxic effect on hFOBs [30] and can stimulate the osteogenic differentiation of rat-derived bone marrow stromal cells [95]. The augmented amount of adsorbed proteins can have a role in this behaviour. At last, Ti64(HF-H_2O_2) has proven to elicit BJ2 human fibroblast adhesion and motility and to reduce the pro-inflammatory activity of THP1 derived macrophages compared to untreated Ti64 [96]. Furthermore, the treated surface showed anti-adhesive behavior toward both Gram-negative and Gram-positive bacteria [42]. Increased albumin adsorption may account for the reduced bacterial adhesion and the anti-inflammatory effect of the treated surface, while higher fibroblast adhesion can be correlated with a higher number of RGD binding sequences exposed by denatured fibronectin. Further studies must be carried out to directly compare these surface treatments in terms of cell response, for the evaluation of the effect of the different adsorption properties. This topic will be object of a comprehensive future investigation, already partially undertaken by the authors of the present paper.

Unfortunately, FTIR analysis of the protein secondary structure has demonstrated some limitations, due to the presence of strong interfering bands because of the OH groups on the surfaces, as already reported by the authors [67]. This is an issue that needs to be addressed in future studies, since biomedical materials are often designed specifically for having a hydroxylated surface [4].

Table 5
Secondary structure of albumin and fibronectin after adsorption on the modified titanium surfaces.

	β-sheets/ turns	α-helix	random coils	β-sheets
	1660–1680	**1650–1660**	**1640–1650**	**1620–1640**
BSA	–	100%	–	–
BSA_h	5%	66%	–	29%
Ti(A-HC-H)_BSA	38%	62%	–	–
Ti64(SrAg)_BSA	24%	76%	–	–
Ti64(HF-H2O2) _BSA	39%	–	61%	–
FN	30%	–	55%	15%
FN_h	40%	–	47%	13%
Ti(A-HC-H)_FN	30%	–	70%	–
Ti64(SrAg)_FN	39%	–	61%	–
Ti64(HF-H2O2) _FN	18%	–	–	82%

4. Conclusion

In this work, the adsorption of albumin and fibronectin, two of the most abundant and relevant proteins in blood serum, has been deeply characterized and investigated on bioactive titanium surfaces, specifically designed for bone contact application. The adsorption process was investigated in conditions as close as possible to the physiological ones, in terms of pH and protein concentrations, which have been rarely

reported since now. Chemical treatments on titanium surfaces greatly enhanced the adsorption of both proteins, thanks to a combined effect of different factors. The presence of a highly porous oxide layer is the major cause of more protein adsorption and, as in the case of Ti(A-HC-H) in comparison with Ti64(HF- H_2O_2), it can overtake the chemical effects such as an augmented SFE or a higher surface hydroxylation degree. Still, the latter two factors have a proven effect on the interactions between the surface and the proteins. Albumin and fibronectin are adsorbed chemically intact and in their zwitterionic form, making a nanometric and homogenous layer on all the surfaces. Their structures, both secondary and tertiary, are affected during the adsorption process, leading to denaturation and conformational changes to different extent depending on the surface they are adsorbed on. In particular, –OH groups play a major role in determining the proteins' secondary structure, according to their amount on the surface and their acidic characteristic.

This work may help to improve the knowledge of the interplay between surface properties, such as porosity, SFE and hydroxylation, and the protein adsorption from biological fluids.

CRediT authorship contribution statement

J. Barberi: Conceptualization, Investigation, Writing – original draft, Writing – review & editing. **L. Mandrile:** Investigation, Methodology, Writing – review & editing. **L. Napione:** Investigation, Methodology, Writing – review & editing. **A.M. Giovannozzi:** Methodology, Writing – review & editing. **A.M. Rossi:** Funding acquisition, Supervision, Writing – review & editing. **A. Vitale:** Investigation, Writing – review & editing. **S. Yamaguchi:** Funding acquisition, Writing – review & editing. **S. Spriano:** Conceptualization, Funding acquisition, Methodology, Supervision, Writing – review & editing.

Declaration of Competing Interest

The authors declare that they have no known competing financial interests or personal relationships that could have appeared to influence the work reported in this paper.

Acknowledgements

This research was in part performed in the IMPreSA Infrastructure laboratories, funded by Regione Piemonte and INRIM. This research did not receive any specific grant from funding agencies in the public, commercial, or not-for-profit sectors. Centro Interdipartimentale Polito BioMEDLab is acknowledged for supporting the measurements by the laser confocal microscope.

Appendix A. Supplementary material

Supplementary data to this article can be found online at https://doi.org/10.1016/j.apsusc.2022.154023.

References

[1] J. Quinn, R. McFadden, C.W. Chan, L. Carson, Titanium for Orthopedic Applications: An Overview of Surface Modification to Improve Biocompatibility and Prevent Bacterial Biofilm Formation, IScience. 23 (2020) 101745, https://doi.org/10.1016/j.isci.2020.101745.

[2] M. Textor, C. Sittig, V. Frauchiger, S. Tosatti, D. Brunette, Properties and Biological Significance of Natural Oxide Films on Titanium and Its Alloys, in: D.M. Brunette, P. Tengvall, M. Textor, P. Thomsen (Eds.), Titan. Med., 1st ed., Springer-Verlag Berlin Heidelberg, Berlin, Heidelberg, 2001.

[3] S. Spriano, S. Yamaguchi, F. Baino, S. Ferraris, A critical review of multifunctional titanium surfaces: New frontiers for improving osseointegration and host response, avoiding bacteria contamination, Acta Biomater. 79 (2018) 1–22, https://doi.org/10.1016/j.actbio.2018.08.013.

[4] T. Hanawa, Titanium-tissue interface reaction and its control with surface treatment, Front. Bioeng. Biotechnol. 7 (2019), https://doi.org/10.3389/fbioe.2019.00170.

[5] D. Buser, S.F.M. Janner, J.G. Wittneben, U. Brägger, C.A. Ramseier, G.E. Salvi, 10-Year Survival and Success Rates of 511 Titanium Implants with a Sandblasted and Acid-Etched Surface: A Retrospective Study in 303 Partially Edentulous Patients, Clin. Implant Dent. Relat. Res. 14 (2012) 839–851, https://doi.org/10.1111/j.1708-8208.2012.00456.x.

[6] J. Barberi, S. Spriano, Titanium and Protein Adsorption: An Overview of Mechanisms and Effects of Surface Features, Materials (Basel) 14 (2021) 1590, https://doi.org/10.3390/ma14071590.

[7] R.M. Visalakshan, M.N. Macgregor, S. Sasidharan, A. Ghazaryan, A. M. Mierczynska-Vasilev, S. Morsbach, V. Mailänder, K. Landfester, J.D. Hayball, K. Vasilev, Biomaterial Surface Hydrophobicity-Mediated Serum Protein Adsorption and Immune Responses, ACS Appl. Mater. Interfaces. 11 (2019) 27615–27623, https://doi.org/10.1021/acsami.9b09900.

[8] K. Nakanishi, T. Sakiyama, K. Imamura, On the adsorption of proteins on solid surfaces, a common but very complicated phenomenon, J. Biosci. Bioeng. 91 (2001) 233–244, https://doi.org/10.1016/S1389-1723(01)80127-4.

[9] W. Norde, My voyage of discovery to proteins in flatland ...and beyond, Colloids Surfaces B Biointerfaces. 61 (2008) 1–9, https://doi.org/10.1016/j.colsurfb.2007.09.029.

[10] T.S. Tsapikouni, Y.F. Missirlis, Protein–material interactions: From micro-to-nano scale, Mater. Sci. Eng. B. 152 (2008) 2–7, https://doi.org/10.1016/j.mseb.2008.06.007.

[11] M. Rabe, D. Verdes, S. Seeger, Understanding protein adsorption phenomena at solid surfaces, Adv. Colloid Interface Sci. 162 (2011) 87–106, https://doi.org/10.1016/j.cis.2010.12.007.

[12] E.A. Vogler, Protein adsorption in three dimensions, Biomaterials. 33 (2012) 1201–1237, https://doi.org/10.1016/j.biomaterials.2011.10.059.

[13] B.S. Kopf, S. Ruch, S. Berner, N.D. Spencer, K. Maniura-Weber, The role of nanostructures and hydrophilicity in osseointegration: In-vitro protein-adsorption and blood-interaction studies, J. Biomed. Mater. Res. Part A. 103 (2015) 2661–2672, https://doi.org/10.1002/jbm.a.35401.

[14] Y. Huang, G. Zha, Q. Luo, J. Zhang, F. Zhang, X. Li, S. Zhao, W. Zhu, X. Li, The construction of hierarchical structure on Ti substrate with superior osteogenic activity and intrinsic antibacterial capability, Sci. Rep. 4 (2015) 6172, https://doi.org/10.1038/srep06172.

[15] X. Lu, S. Xiong, Y. Chen, F. Zhao, Y. Hu, Y. Guo, B. Wu, P. Huang, B. Yang, Effects of statherin on the biological properties of titanium metals subjected to different surface modification, Colloids Surfaces B Biointerfaces. 188 (2020) 110783, https://doi.org/10.1016/j.colsurfb.2020.110783.

[16] O.R. Cámara, L.B. Avalle, F.Y. Oliva, Protein adsorption on titanium dioxide: Effects on double layer and semiconductor space charge region studied by EIS, Electrochim. Acta. 55 (2010) 4519–4528, https://doi.org/10.1016/j.electacta.2010.03.003.

[17] K. Imamura, M. Shimomura, S. Nagai, M. Akamatsu, K. Nakanishi, Adsorption characteristics of various proteins to a titanium surface, J. Biosci. Bioeng. 106 (2008) 273–278, https://doi.org/10.1263/jbb.106.273.

[18] M. Pegueroles, A. Aguirre, E. Engel, G. Pavon, F.J. Gil, J.A. Planell, V. Migonney, C. Aparicio, Effect of blasting treatment and Fn coating on MG63 adhesion and differentiation on titanium: A gene expression study using real-time RT-PCR, J. Mater. Sci. Mater. Med. 22 (2011) 617–627, https://doi.org/10.1007/s10856-011-4229-3.

[19] F. Mussano, T. Genova, M. Laurenti, D. Gaglioti, G. Scarpellino, P. Rivolo, M. G. Faga, P.A. Fiorio, L. Munaron, P. Mandracci, S. Carossa, Beta1-integrin and TRPV4 are involved in osteoblast adhesion to different titanium surface topographies, Appl. Surf. Sci. 507 (2020) 145112, https://doi.org/10.1016/j.apsusc.2019.145112.

[20] C. Herranz-Diez, F. Gil, J. Guillem-Marti, J. Manero, Mechanical and physicochemical characterization along with biological interactions of a new Ti25Nb21Hf alloy for bone tissue engineering, J. Biomater. Appl. 30 (2015) 171–181, https://doi.org/10.1177/0885328215577524.

[21] A. Michiardi, C. Aparicio, B.D. Ratner, J.A. Planell, J. Gil, The influence of surface energy on competitive protein adsorption on oxidized NiTi surfaces, Biomaterials. 28 (2007) 586–594, https://doi.org/10.1016/j.biomaterials.2006.09.040.

[22] N. Hori, T. Ueno, H. Minamikawa, F. Iwasa, F. Yoshino, K. Kimoto, M.C. Il Lee, T. Ogawa, Electrostatic control of protein adsorption on UV-photofunctionalized titanium, Acta Biomater. 6 (2010) 4175–4180, https://doi.org/10.1016/j.actbio.2010.05.006.

[23] Y. Li, Y. Dong, Y. Zhang, Y. Yang, R. Hu, P. Mu, X. Liu, C. Lin, Q. Huang, Synergistic effect of crystalline phase on protein adsorption and cell behaviors on TiO2 nanotubes, Appl. Nanosci. 10 (2020) 3245–3257, https://doi.org/10.1007/s13204-019-01078-2.

[24] Q. Yang, Y. Zhang, M. Liu, M. Ye, Y. Zhang, S. Yao, Study of fibrinogen adsorption on hydroxyapatite and TiO2 surfaces by electrochemical piezoelectric quartz crystal impedance and FTIR–ATR spectroscopy, Anal. Chim. Acta. 597 (2007) 58–66, https://doi.org/10.1016/j.aca.2007.06.025.

[25] A.G. Hemmersam, K. Rechendorff, M. Foss, D.S. Sutherland, F. Besenbacher, Fibronectin adsorption on gold, Ti-, and Ta-oxide investigated by QCM-D and RSA modelling, J. Colloid Interface Sci. 320 (2008) 110–116, https://doi.org/10.1016/j.jcis.2007.11.047.

[26] L. Canullo, T. Genova, M. Tallarico, G. Gautier, F. Mussano, D. Botticelli, Plasma of Argon Affects the Earliest Biological Response of Different Implant Surfaces, J. Dent. Res. 95 (2016) 566–573, https://doi.org/10.1177/0022034516629119.

[27] E. Migliorini, M. Weidenhaupt, C. Picart, Practical guide to characterize biomolecule adsorption on solid surfaces (Review), Biointerphases. 13 (2018) 06D303, https://doi.org/10.1116/1.5045122.

[28] K. Zheng, M. Kapp, A.R. Boccaccini, Protein interactions with bioactive glass surfaces: A review, Appl. Mater. Today. 15 (2019) 350–371, https://doi.org/10.1016/j.apmt.2019.02.003.

[29] D.K. Pattanayak, S. Yamaguchi, T. Matsushita, T. Kokubo, Effect of heat treatments on apatite-forming ability of NaOH- and HCl-treated titanium metal, J. Mater. Sci. Mater. Med. 22 (2011) 273–278, https://doi.org/10.1007/s10856-010-4218-y.

[30] S. Yamaguchi, P.T. Minh Le, M. Ito, S.A. Shintani, H. Takadama, Tri-functional calcium-deficient calcium titanate coating on titanium metal by chemical and heat treatment, Coatings. 9 (2019), https://doi.org/10.3390/coatings9090561.

[31] S. Ferraris, S. Spriano, G. Pan, A. Venturello, C.L. Bianchi, R. Chiesa, M.G. Faga, G. Maina, E. Vernè, Surface modification of Ti–6Al–4V alloy for biomineralization and specific biological response: Part I, inorganic modification, J. Mater. Sci. Mater. Med. 22 (2011) 533–545, https://doi.org/10.1007/s10856-011-4246-2.

[32] A.M. Merlot, D.S. Kalinowski, D.R. Richardson, Unraveling the mysteries of serum albumin-more than just a serum protein, Front. Physiol. 5 AUG (2014) 1–7. 10.3389/fphys.2014.00299.

[33] E. Österlund, The secondary structure of human plasma fibronectin: conformational changes induced by acidic pH and elevated temperatures; a circular dichroic study, Biochim. Biophys. Acta (BBA)/Protein Struct. Mol. 955 (1988) 330–336, https://doi.org/10.1016/0167-4838(88)90212-9.

[34] A. Rudawska, E. Jacniacka, Analysis for determining surface free energy uncertainty by the Owen-Wendt method, Int. J. Adhes. Adhes. 29 (2009) 451–457, https://doi.org/10.1016/j.ijadhadh.2008.09.008.

[35] S. Ferraris, S. Yamaguchi, N. Barbani, M. Cazzola, C. Cristallini, M. Miola, E. Vernè, S. Spriano, Bioactive materials: In vitro investigation of different mechanisms of hydroxyapatite precipitation, Acta Biomater. 102 (2020) 468–480, https://doi.org/10.1016/j.actbio.2019.11.024.

[36] J.S. Stevens, A.C. De Luca, M. Pelendritis, G. Terenghi, S. Downes, S.L. M. Schroeder, Quantitative analysis of complex amino acids and RGD peptides by X-ray photoelectron spectroscopy (XPS), Surf. Interface Anal. 45 (2013) 1238–1246, https://doi.org/10.1002/sia.5261.

[37] A. Vallée, V. Humblot, R. Al Housseiny, S. Boujday, C.M. Pradier, BSA adsorption on aliphatic and aromatic acid SAMs: Investigating the effect of residual surface charge and sublayer nature, Colloids Surfaces B Biointerfaces. 109 (2013) 136–142, https://doi.org/10.1016/j.colsurfb.2013.03.014.

[38] K.S. Siow, L. Britcher, S. Kumar, H.J. Griesser, QCM-D and XPS study of protein adsorption on plasma polymers with sulfonate and phosphonate surface groups, Colloids Surfaces B Biointerfaces. 173 (2019) 447–453, https://doi.org/10.1016/j.colsurfb.2018.10.015.

[39] A. Shchukarev, B.Ö. Malekzadeh, M. Ransjö, P. Tengvall, A. Westerlund, Surface characterization of insulin-coated Ti6Al4V medical implants conditioned in cell culture medium: An XPS study, J. Electron Spectros. Relat. Phenomena. 216 (2017) 33–38, https://doi.org/10.1016/j.elspec.2017.03.001.

[40] D. Nečas, P. Klapetek, Gwyddion: an open-source software for SPM data analysis, Open Phys. 10 (2012) 181–188, https://doi.org/10.2478/s11534-011-0096-2.

[41] S. Ferraris, M. Cazzola, V. Peretti, B. Stella, S. Spriano, Zeta potential measurements on solid surfaces for in Vitro biomaterials testing: Surface charge, reactivity upon contact with fluids and protein absorption, Front. Bioeng Biotechnol. 6 (2018) 1–7, https://doi.org/10.3389/fbioe.2018.00060.

[42] S. Ferraris, A. Cochis, M. Cazzola, M. Tortello, A. Scalia, S. Spriano, L. Rimondini, Cytocompatible and Anti-bacterial Adhesion Nanotextured Titanium Oxide Layer on Titanium Surfaces for Dental and Orthopedic Implants, Front. Bioeng. Biotechnol. 7 (2019) 1–12, https://doi.org/10.3389/fbioe.2019.00103.

[43] A. Cochis, J. Barberi, S. Ferraris, M. Miola, L. Rimondini, E. Vernè, S. Yamaguchi, S. Spriano, Competitive Surface Colonization of Antibacterial and Bioactive Materials Doped with Strontium and/or Silver Ions, Nanomaterials. 10 (2020) 120, https://doi.org/10.3390/nano10010120.

[44] M. Caneva, N.P. Lang, J.L. Calvo Guirado, S. Spriano, G. Iezzi, D. Botticelli, Bone healing at bicortically installed implants with different surface configurations. An experimental study in rabbits, Clin. Oral Implants Res. 26 (2015) 293–299, https://doi.org/10.1111/clr.12475.

[45] S. Ferraris, S. Yamaguchi, N. Barbani, C. Cristallini, G. Gautier di Confiengo, J. Barberi, M. Cazzola, M. Miola, E. Vernè, S. Spriano, The mechanical and chemical stability of the interfaces in bioactive materials: The substrate-bioactive surface layer and hydroxyapatite-bioactive surface layer interfaces, Mater. Sci. Eng. C. 116 (2020) 111238, https://doi.org/10.1016/j.msec.2020.111238.

[46] S.-H. Choi, J.-H. Ryu, J.-S. Kwon, J.-E. Kim, J.-Y. Cha, K.-J. Lee, H.-S. Yu, E.-H. Choi, K.-M. Kim, C.-J. Hwang, Effect of wet storage on the bioactivity of ultraviolet light- and non-thermal atmospheric pressure plasma-treated titanium and zirconia implant surfaces, Mater. Sci. Eng. C. 105 (2019) 110049, https://doi.org/10.1016/j.msec.2019.110049.

[47] L. Burgos-Asperilla, M.C. García-Alonso, M.L. Escudero, C. Alonso, Study of the interaction of inorganic and organic compounds of cell culture medium with a Ti surface, Acta Biomater. 6 (2010) 652–661, https://doi.org/10.1016/j.actbio.2009.06.019.

[48] M.C. Biesinger, L.W.M. Lau, A.R. Gerson, R.S.C. Smart, Resolving surface chemical states in XPS analysis of first row transition metals, oxides and hydroxides: Sc, Ti, V, Cu and Zn, Appl. Surf. Sci. 257 (2010) 887–898, https://doi.org/10.1016/j.apsusc.2010.07.086.

[49] K. Song, J. Lee, S.O. Choi, J. Kim, Interaction of surface energy components between solid and liquid on wettabilit, Polymers (Basel). 11 (2019), https://doi.org/10.3390/polym11030498.

[50] B.S. Bal, M.N. Rahaman, Orthopedic applications of silicon nitride ceramics, Acta Biomater. 8 (2012) 2889–2898, https://doi.org/10.1016/j.actbio.2012.04.031.

[51] X. Shi, K. Tsuru, L. Xu, G. Kawachi, K. Ishikawa, Effects of solution pH on the structure and biocompatibility of Mg-containing TiO 2 layer fabricated on titanium by hydrothermal treatment, Appl. Surf. Sci. 270 (2013) 445–451, https://doi.org/10.1016/j.apsusc.2013.01.046.

[52] C. Gruian, E. Vanea, S. Simon, V. Simon, FTIR and XPS studies of protein adsorption onto functionalized bioactive glass, Biochim. Biophys. Acta - Proteins Proteomics. 2012 (1824) 873–881, https://doi.org/10.1016/j.bbapap.2012.04.008.

[53] J. Shi, B. Feng, X. Lu, J. Weng, Adsorption of bovine serum albumin onto titanium dioxide nanotube arrays, Int. J. Mater. Res. 103 (2012) 889–896, https://doi.org/10.3139/146.110696.

[54] R.N. Foster, E.T. Harrison, D.G. Castner, ToF-SIMS and XPS Characterization of Protein Films Adsorbed onto Bare and Sodium Styrenesulfonate-Grafted Gold Substrates, Langmuir. 32 (2016) 3207–3216, https://doi.org/10.1021/acs.langmuir.5b04743.

[55] X.N. Hu, B.C. Yang, Conformation change of bovine serum albumin induced by bioactive titanium metals and its effects on cell behaviors, J. Biomed. Mater. Res. - Part A. 102 (2014) 1053–1062, https://doi.org/10.1002/jbm.a.34768.

[56] M.N. Biao, Y.M. Chen, S.B. Xiong, B.Y. Wu, B.C. Yang, Synergistic effects of fibronectin and bone morphogenetic protein on the bioactivity of titanium metal, J. Biomed. Mater. Res. - Part A. 105 (2017) 2485–2498, https://doi.org/10.1002/jbm.a.36106.

[57] Y.S. Hedberg, M.S. Killian, E. Blomberg, S. Virtanen, P. Schmuki, I. Odnevall Wallinder, Interaction of Bovine Serum Albumin and Lysozyme with Stainless Steel Studied by Time-of-Flight Secondary Ion Mass Spectrometry and X-ray Photoelectron Spectroscopy, Langmuir 28 (2012) 16306–16317, https://doi.org/10.1021/la3039279.

[58] V.V.D. Rani, K. Manzoor, D. Menon, N. Selvamurugan, S.V. Nair, The design of novel nanostructures on titanium by solution chemistry for an improved osteoblast response, Nanotechnology. 20 (2009), https://doi.org/10.1088/0957-4484/20/19/195101.

[59] E.A. dos Santos, M. Farina, G.A. Soares, K. Anselme, Surface energy of hydroxyapatite and β-tricalcium phosphate ceramics driving serum protein adsorption and osteoblast adhesion, J. Mater. Sci. Mater. Med. 19 (2008) 2307–2316, https://doi.org/10.1007/s10856-007-3347-4.

[60] K. Zhou, J. Chen, T. Wang, Y. Su, L. Qiao, Y. Yan, Effect of surface energy on protein adsorption behaviours of treated CoCrMo alloy surfaces, Appl. Surf. Sci. 520 (2020) 146354, https://doi.org/10.1016/j.apsusc.2020.146354.

[61] Y. Yoneyama, T. Matsuno, Y. Hashimoto, T. Satoh, In vitro evaluation of H2O2 hydrothermal treatment of aged titanium surface to enhance biofunctional activity, Dent. Mater. J. 32 (2013) 115–121, https://doi.org/10.4012/dmj.2012-087.

[62] K. Magyari, C. Gruian, B. Varga, R. Ciceo-Lucacel, T. Radu, H.J. Steinhoff, G. Váró, V. Simon, L. Baia, Addressing the optimal silver content in bioactive glass systems in terms of BSA adsorption, J. Mater. Chem. B. 2 (2014) 5799–5808, https://doi.org/10.1039/c4tb00733f.

[63] F. Romero-Gavilán, N. Araújo-Gomes, I. García-Arnáez, C. Martínez-Ramos, F. Elortza, M. Azkargorta, I. Iloro, M. Gurruchaga, J. Suay, I. Goñi, The effect of strontium incorporation into sol-gel biomaterials on their protein adsorption and cell interactions, Colloids Surfaces B Biointerfaces. 174 (2019) 9–16, https://doi.org/10.1016/j.colsurfb.2018.10.075.

[64] K. Nam, K. Eom, J. Yang, J. Park, G. Lee, K. Jang, H. Lee, S.W. Lee, D.S. Yoon, C. Y. Lee, T. Kwon, Aptamer-functionalized nano-pattern based on carbon nanotube for sensitive, selective protein detection, J. Mater. Chem. 22 (2012) 23348–23356, https://doi.org/10.1039/c2jm33688j.

[65] H. Lee, S.W. Lee, G. Lee, W. Lee, K. Nam, J.H. Lee, K.S. Hwang, J. Yang, H. Lee, S. Kim, S.W. Lee, D.S. Yoon, Identifying DNA mismatches at single-nucleotide resolution by probing individual surface potentials of DNA-capped nanoparticles, Nanoscale. 10 (2018) 538–547, https://doi.org/10.1039/C7NR05250B.

[66] E. Rahimi, R. Offoiach, K. Baert, H. Terryn, M. Lekka, L. Fedrizzi, Role of phosphate, calcium species and hydrogen peroxide on albumin protein adsorption on surface oxide of Ti6Al4V alloy, Materialia. 15 (2021), https://doi.org/10.1016/j.mtla.2020.100988.

[67] J. Barberi, S. Ferraris, A.M. Giovannozzi, L. Mandrile, E. Piatti, A.M. Rossi, S. Spriano, Advanced characterization of albumin adsorption on a chemically treated surface for osseointegration: An innovative experimental approach, Mater. Des. 218 (2022) 110712, https://doi.org/10.1016/j.matdes.2022.110712.

[68] S. Kashiwaya, J. Morasch, V. Streibel, T. Toupance, W. Jaegermann, A. Klein, The Work Function of TiO2, Surfaces. 1 (2018) 73–89, https://doi.org/10.3390/surfaces1010007.

[69] A. Ithurbide, I. Frateur, A. Galtayries, P. Marcus, XPS and flow-cell EQCM study of albumin adsorption on passivated chromium surfaces: Influence of potential and pH, Electrochim. Acta. 53 (2007) 1336–1345, https://doi.org/10.1016/j.electacta.2007.04.109.

[70] V. Payet, T. Dini, S. Brunner, A. Galtayries, I. Frateur, P. Marcus, Pre-treatment of titanium surfaces by fibronectin: In situ adsorption and effect of concentration, Surf. Interface Anal. 42 (2010) 457–461, https://doi.org/10.1002/sia.3298.

[71] M.M. Shalabi, A. Gortemaker, M.A. Van't Hof, J.A. Jansen, N.H.J. Creugers, Implant surface roughness and bone healing: A systematic review, J. Dent. Res. 85 (2006) 496–500. 10.1177/154405910608500603.

[72] A. Sadana, Enzyme Deactivation in Reactors, Biocatalysis. 2 (1989) 175–216, https://doi.org/10.3109/10242428909035033.

[73] I. Wierzbicka-Patynowski, J.E. Schwarzbauer, The ins and outs of fibronectin matrix assembly, J. Cell Sci. 116 (2003) 3269–3276, https://doi.org/10.1242/jcs.00670.

[74] N.E. Muzzio, M.A. Pasquale, X. Rios, O. Azzaroni, J. Llop, S.E. Moya, Adsorption and Exchangeability of Fibronectin and Serum Albumin Protein Corona on Annealed Polyelectrolyte Multilayers and Their Consequences on Cell Adhesion, Adv. Mater. Interfaces. 6 (2019), https://doi.org/10.1002/admi.201900008.

[75] K. Imamura, M. Oshita, M. Iwai, T. Kuroda, I. Watanabe, T. Sakiyama, K. Nakanishi, Influences of properties of protein and adsorption surface on removal kinetics of protein adsorbed on metal surface by H2O2-electrolysis treatment, J. Colloid Interface Sci. 345 (2010) 474–480, https://doi.org/10.1016/j.jcis.2010.01.083.
[76] T. Peters, All About Albumin, Elsevier (1995), https://doi.org/10.1016/B978-0-12-552110-9.X5000-4.
[77] S. Fujibayashi, T. Nakamura, S. Nishiguchi, J. Tamura, M. Uchida, H.-M. Kim, T. Kokubo, Bioactive titanium: Effect of sodium removal on the bone-bonding ability of bioactive titanium prepared by alkali and heat treatment, J. Biomed. Mater. Res. 56 (2001) 562–570, https://doi.org/10.1002/1097-4636(20010915)56:4<562::AID-JBM1128>3.0.CO;2-M.
[78] R. Li, Z. Wu, Y. Wangb, L. Ding, Y. Wang, Role of pH-induced structural change in protein aggregation in foam fractionation of bovine serum albumin, Biotechnol. Reports. 9 (2016) 46–52, https://doi.org/10.1016/j.btre.2016.01.002.
[79] T. Luxbacher, The zeta potential for solid surface analysis, Anton Paar GmbH, 2014.
[80] C.F. Wertz, M.M. Santore, Effect of Surface Hydrophobicity on Adsorption and Relaxation Kinetics of Albumin and Fibrinogen: Single-Species and Competitive Behavior, Langmuir. 17 (2001) 3006–3016, https://doi.org/10.1021/la0017781.
[81] E. Peyrin, Y.C. Guillaume, C. Guinchard, Characterization of solute binding at human serum albumin site II and its geometry using a biochromatographic approach, Biophys. J. 77 (1999) 1206–1212, https://doi.org/10.1016/S0006-3495(99)76972-9.
[82] M. Bergkvist, J. Carlsson, S. Oscarsson, Surface-dependent conformations of human plasma fibronectin adsorbed to silica, mica, and hydrophobic surfaces, studied with use of Atomic Force Microscopy, J. Biomed. Mater. Res. - Part A. 64 (2003) 349–356, https://doi.org/10.1002/jbm.a.10423.
[83] L. Parisi, A. Toffoli, B. Ghezzi, B. Mozzoni, S. Lumetti, G.M. Macaluso, A glance on the role of fibronectin in controlling cell response at biomaterial interface, Jpn. Dent. Sci. Rev. 56 (2020) 50–55, https://doi.org/10.1016/j.jdsr.2019.11.002.
[84] S. Damodaran, K.L. Parkin, Fennema's Food Chemistry, Fifth Edition, CRC Press, 2017. 10.1201/9781315372914.
[85] V. Vadillo-Rodríguez, M.A. Pacha-Olivenza, M.L. Gõnzalez-Martín, J.M. Bruque, A. M. Gallardo-Moreno, M.L. Gónzalez-Martín, J.M. Bruque, A.M. Gallardo-Moreno, Adsorption behavior of human plasma fibronectin on hydrophobic and hydrophilic Ti6Al4V substrata and its influence on bacterial adhesion and detachment, J. Biomed. Mater. Res. - Part A. 101 A (2013) 1397–1404. 10.1002/jbm.a.34447.
[86] A. Barth, Infrared spectroscopy of proteins, Biochim. Biophys. Acta - Bioenerg. 1767 (2007) 1073–1101, https://doi.org/10.1016/j.bbabio.2007.06.004.
[87] M. Xiao, M. Biao, Y. Chen, M. Xie, B. Yang, Regulating the osteogenic function of rhBMP 2 by different titanium surface properties, J. Biomed. Mater. Res. Part A. 104 (2016) 1882–1893, https://doi.org/10.1002/jbm.a.35719.
[88] M.Z. Mughal, P. Lemoine, G. Lubarsky, P.D. Maguire, Protein adsorption on nano-patterned hydrogenated amorphous carbon model surfaces, Mater. Des. 97 (2016) 239–248, https://doi.org/10.1016/j.matdes.2016.02.043.
[89] Z. Xu, V.H. Grassian, Bovine serum albumin adsorption on TiO2 nanoparticle surfaces: Effects of ph and coadsorption of phosphate on protein-surface interactions and protein structure, J. Phys. Chem. C. 121 (2017) 21763–21771, https://doi.org/10.1021/acs.jpcc.7b07525.
[90] M. Jackson, H.H. Mantsch, The use and misuse of FTIR spectroscopy in the determination of protein structure, Crit. Rev. Biochem. Mol. Biol. 30 (1995) 95–120, https://doi.org/10.3109/10409239509085140.
[91] A. Gand, M. Tabuteau, C. Chat, G. Ladam, H. Atmani, P.R. Van Tassel, E. Pauthe, Fibronectin-based multilayer thin films, Colloids Surfaces B Biointerfaces. 156 (2017) 313–319, https://doi.org/10.1016/j.colsurfb.2017.05.023.
[92] H. Yamazoe, Spectroscopic study on the conformation of serum albumin in film state, J. Biosci. Bioeng. 127 (2019) 515–519, https://doi.org/10.1016/j.jbiosc.2018.09.015.
[93] L.M. Szott, T.A. Horbett, Protein interactions with surfaces: cellular responses, complement activation, and newer methods, Curr. Opin. Chem. Biol. 15 (2011) 677–682, https://doi.org/10.1016/j.cbpa.2011.04.021.
[94] T. Kawai, M. Takemoto, S. Fujibayashi, M. Neo, H. Akiyama, S. Yamaguchi, D. K. Pattanayak, T. Matsushita, T. Nakamura, T. Kokubo, Bone-bonding properties of Ti metal subjected to acid and heat treatments, J. Mater. Sci. Mater. Med. 23 (2012) 2981–2992, https://doi.org/10.1007/s10856-012-4758-4.
[95] Y. Okuzu, S. Fujibayashi, S. Yamaguchi, K. Masamoto, B. Otsuki, K. Goto, T. Kawai, T. Shimizu, K. Morizane, T. Kawata, Y. Shimizu, M. Hayashi, S. Matsuda, In vitro study of antibacterial and osteogenic activity of titanium metal releasing strontium and silver ions, J. Biomater. Appl. 35 (2021) 670–680, https://doi.org/10.1177/0885328220959584.
[96] J. Barthes, M. Cazzola, C. Muller, C. Dollinger, C. Debry, S. Ferraris, S. Spriano, N. E. Vrana, Controlling porous titanium/soft tissue interactions with an innovative surface chemical treatment: Responses of macrophages and fibroblasts, Mater. Sci. Eng. C. 112 (2020) 110845, https://doi.org/10.1016/j.msec.2020.110845.